This article has been accepted for publication in a future issue of this journal, but has not been fully edited. Content may change prior to final publication. Citation information: DOI 10.1109/TAC.2019.2927708, IEEE Transactions on Automatic Control

Hybrid Control for Robust and Global Tracking on Smooth Manifolds

Pedro Casau, Rita Cunha, Ricardo G. Sanfelice and Carlos Silvestre

***Abstract*—n this paper, we present a hybrid control strategy that allows for global asymptotic tracking of reference trajectories evolving on smooth manifolds, with nominal robustness. Two different versions of the hybrid controller are presented: one which allows for discontinuities of the plant input and a second one that removes the discontinuities via dynamic extension.n this paper, we present a hybrid control strategy that allows for global asymptotic tracking of reference trajectories evolving on smooth manifolds, with nominal robustness. Two different versions of the hybrid controller are presented: one which allows for discontinuities of the plant input and a second one that removes the discontinuities via dynamic extension.I that live in the given manifold. By taking an exosystem approach, we provide a general construction of a hybrid controller that guarantees global asymptotic stability of the zero tracking error set. The proposed construction relies on the existence of proper indicators and a transport map-like function for the given manifold. We provide a construction of these functions for the case where each chart in a smooth atlas for the manifold maps its domain onto the Euclidean space. We also provide conditions for exponential convergence to the zero tracking error set. To illustrate these properties, the proposed controller is exercised on three different compact manifolds – the two-dimensional sphere, the unit-quaternion group and the special orthogonal group of order three – and further applied to the problems of obstacle avoidance in the plane and global synchronization on the circle.**

I. Introduction

A. Background and Motivation

In this paper, we consider the problem of designing a controller that performs asymptotic tracking of a given reference trajectory for a dynamical system evolving on a smooth manifold without boundary, robustly with respect to small measurement noise and globally with respect to initial conditions. The design of such controllers is particularly relevant in robotics, because there are several mechanical systems that have components whose movement is constrained to a manifold. For example, spacecraft, aircraft, rotorcraft and underwater vehicles are described as rigid-bodies whose orientation in three dimensional space is represented by a 3×3 nonsingular matrix R satisfying $R^\top = R^{-1}$ and $\det(R) = 1$ which defines a compact manifold of dimension 3 and together with matrix multiplication forms the special orthogonal group of order three $\mathsf{SO}(3)$ (c.f. [1], [2]). Vectored-thrust vehicles are aerial vehicles with full torque actuation and a single force direction (thrust) which often resort to controllers for asymptotic tracking on the sphere, denoted by $\mathbb{S}^2$, in order to steer the thrust vector in a desired direction (see e.g. [3], [4], [5]). Surface vessels are rigid-body vehicles that move on the plane and have a single rotational degree of freedom, hence their attitude can be represented by an element of the circle, denoted by $\mathbb{S}^1$ (see e.g. [6], [7]). Robotic manipulators are composed of a series of links connected by joints whose state can be described as an element of $\mathbb{S}^1$, $\mathbb{S}^2$ or $\mathsf{SO}(3)$ depending on the particular kind of joint (c.f. [8]). Naturally, control problems that involve one or more of these robots are described partly in compact manifolds. For example, spacecraft docking and formation control require the synchronization of multiple rigid-body vehicles and the dynamical system that characterizes the relative orientation between vehicles also evolves on a compact manifold (see [9] and [10]). Obstacle avoidance is another important and longstanding problem in robotics that reflects the need to drive mechanical systems from one place to another while avoiding any number of obstacles in its way, which constrains the state space to a submanifold of the original space. Several solutions to this problem have been proposed over the last few decades as highlighted in [11].

Designing controllers that guarantee robust and global tracking for manifolds is challenging and, generally, an unsolved problem. In the next section, we revisit existing control strategies that could potentially be used to tackle the problem at hand and highlight their limitations.

B. Related Work

It was shown in [12] that asymptotic controllability implies feedback stabilizability of the origin of a nonlinear dynamical system

$$\dot{x} = f(x, u)$$

with state $x \in \mathscr{M}$ and input $u \in \mathbb{U}$, where $\mathscr{M}$ is a smooth manifold that is embedded in a higher dimensional Euclidean space and $\mathbb{U}$ a locally compact metric space. In other words, one needs only to verify controllability, that the existence of a stabilizing feedback law immediately follows. Unfortunately, the aforementioned result is not constructive, hence, to find control synthesis procedures, one has to look into particular classes of nonlinear systems.

P. Casau and C. Silvestre are with the Department of Electrical and Computer Engineering of the Faculty of Science and Technology of the University of Macau, Macau, China, and with Instituto Superior Técnico, Universidade de Lisboa, Lisboa, Portugal. This work was partially supported by the projects MYRG2018-00198-FST and MYRG2016-00097-FST of the University of Macau; by the Macau Science and Technology, Development Fund under Grant FDCT/026/2017/A1 and by Fundação para a Ciência e a Tecnologia (FCT) through Project UID/EEA/50009/2019, and LOTUS PTDC/EEI-AUT/5048/2014 and grant CEECIND/04652/2017. Research by R. G. Sanfelice partially supported by NSF Grants no. ECS-1710621 and CNS-1544396, by AFOSR Grants no. FA9550-16-1-0015, FA9550-19-1-0053, and FA9550-19-1-0169, and by CITRIS and the Banatao Institute at the University of California.

This article has been accepted for publication in a future issue of this journal, but has not been fully edited. Content may change prior to final publication. Citation information: DOI 10.1109/TAC.2019.2927708, IEEE Transactions on Automatic Control

In the particular case of control affine systems of the form

$$\dot{x} = f(x) + g(x)u$$

with smooth functions $f : \mathbb{R}^m \to \mathbb{R}^m$ and $g : \mathbb{R}^n \to \mathbb{R}^{m\times k}$ satisfying $f(0) = 0$, the work reported [13] proposes a static state feedback law $k : \mathbb{R}^m \to \mathbb{R}^k$ that renders the origin of the closed-loop system globally asymptotically stable, provided that there exists a smooth control Lyapunov function, i.e., a positive-definite function V whose derivative is strictly negative everywhere but the origin for some input value. The work in [14] addresses the problem of trajectory tracking for a dynamical system evolving on a Riemannian manifold, under the assumption that there exists a transport map that is compatible with an error function on the manifold. The transport map transfers the velocity of the reference trajectory to the tangent space at the current location, allowing for a direct comparison between the current and the reference velocities. These works follow a Lyapunov approach which is at the heart of nonlinear control design: if a control Lyapunov function exists, then it is possible to construct a feedback law (see, e.g., [15] and [16]). However, finding control Lyapunov functions is not a trivial endeavor and it relies heavily on the experience of the control practitioner. Moreover, even when found, one may not know the basin of attraction for the closed-loop dynamical system, that is, the set of points from which solutions converge.

In this regard, asymptotic stabilization on compact Lie groups, for example, is much simpler. It was shown in [2] that if there exists a Morse function on the given compact Lie group, then it is possible to almost globally stabilize its minimum by gradient descent, in the sense that all trajectories to the closed-loop system converge to the minimum of the function, except for solutions starting on a set of measure zero. Since smooth Morse functions are dense on the space of functions on a manifold [17], it is fairly easy to construct a controller for setpoint stabilization on a Lie group whose basin of attraction is *almost* the entire state space. The work in [2] has had a profound impact in some of the applications that are mentioned in Section I-A, such as: attitude control [18], tracking for robotic manipulators [8], spacecraft stabilization [19] and, more recently, PID control for systems evolving on Lie groups [20]. In addition, geometric controllers for almost global asymptotic stabilization on Lie groups can be smoothly projected onto manifolds that lack the group structure and a natural configuration error (see e.g. [21]). However, these strategies are hindered by a fairly well-known limitation of continuous feedback that has been explicitly stated in [22] as follows: *"a continuous dynamical system on a state space that has the structure of a vector bundle on a compact manifold possesses no globally asymptotically stable equilibrium."* It is possible to tackle this limitation by means of nonsmooth feedback, as done in [23] and [24] for the stabilization of a rigid-body and the 3-D pendulum, respectively. However, even if it is possible to globally asymptotically stabilize a setpoint for systems evolving on compact manifolds by means of discontinuous feedback, this approach is not robust to small measurement noise, as discussed in [25]. In addition, it was shown in [26] that a state space that is punctured with spherical obstacles is also plagued with topological obstructions that preclude global asymptotic stabilization of a setpoint by continuous feedback.

In summary, the main challenges to solve the problem of robust and global trajectory tracking for systems evolving on smooth manifolds are the following:

(L1) The existence of topological obstructions to global asymptotic stabilization on compact manifolds by continuous feedback – the results available in the literature only apply to specific cases of the systems considered here;

(L2) Lack of robustness to measurement noise of smooth and nonsmooth feedback – the unavoidable nonsmoothness of any global stabilizer and the much desired robustness requires the use of advanced hybrid control techniques, which, to date, have been only applied to systems on manifolds with very specific dynamics and manifold structure;

(L3) Constructive controller synthesis for general dynamical systems on manifolds – a "universal" (hybrid or not) control construction for robust and global stabilization of a point or reference of a wide class of systems on manifolds is not available in the literature;

A particular control synthesis tool that emerged to address (L1) and (L2) consists on hybrid control through synergistic potential functions (see e.g. [27], [28], [29] and references therein). These are collections of functions with the following property: for each unstable equilibrium point of the gradient vector field of a given function, there exists another function in the family that has a lower value. By monitoring the difference between the value of the current function and the lowest possible value among all functions in the collection, it is possible to globally asymptotically stabilize a given reference by switching between gradient-based vector fields whenever a given amount is exceeded. This novel hybrid control technique spawned a plethora of contributions on global asymptotic stabilization on compact manifolds, including, most notably, the two-dimensional sphere [30], the three-dimensional sphere [31] and the special orthogonal group [32], [33]. It has also found applications in attitude stabilization [34], rigid-body vehicle stabilization and tracking [35], tracking for quadrotor vehicles [36] and obstacle avoidance [37].

While the aforementioned hybrid control strategies address the limitations that are pointed out in (L1) and (L2), they only apply to very specific examples and are built on a case-by-case basis which depends on the particular application under consideration. One of the contributions of the present paper is precisely the construction of a broad scope controller that can not only be applied to these particular examples, but also to more complex control tasks, possibly while guaranteeing exponential convergence to a reference trajectory, as discussed in the next section.

C. Contributions

Let $\mathscr{M}$ denote a smooth manifold of dimension n without

This article has been accepted for publication in a future issue of this journal, but has not been fully edited. Content may change prior to final publication. Citation information: DOI 10.1109/TAC.2019.2927708, IEEE Transactions on Automatic Control

boundary that is properly embedded in a higher dimensional Euclidean space $\mathbb{R}^m$. In this paper, we design a hybrid controller that globally asymptotically tracks a reference trajectory for the dynamical system

$$\dot{x} = \Pi(x)\omega \tag{1a}$$

$$\dot{\omega} = u \tag{1b}$$

where $x \in \mathscr{M} \subset \mathbb{R}^m$, $\omega \in \mathbb{R}^k$, $u \in \mathbb{R}^k$ denotes the input of the system and $\Pi : \mathbb{R}^m \to \mathbb{R}^{m\times k}$ is a smooth matrix-valued function that satisfies $\mathsf{T}_x\mathscr{M} = \mathrm{Im}(\Pi(x))$ for each $x \in \mathscr{M}$, where $\mathsf{T}_x\mathscr{M}$ denotes the tangent space to $\mathscr{M}$ at x and

$$\mathrm{Im}(\Pi(x)) := \{y \in \mathbb{R}^m : y = \Pi(x)v \text{ for some } v \in \mathbb{R}^k\}$$

is the image of Π at x. Under the previous assumptions, the dimension of the subspace $\mathrm{Im}(\Pi(x))$ is n for each $x \in \mathscr{M}$, therefore the system (1) is a *controllable driftless* dynamical system (c.f., [1]).

The solution to this problem relies on the following key observations. Given a finite collection $\{U_h\}_{h\in\mathcal{N}}$ of open subsets of $\mathscr{M}$ that cover the entire manifold and a collection of functions V_h that are radially unbounded on U_h, we switch from V_h to $V_{h'}$, if the value of V_h exceeds the value of $V_{h'}$ at a point by an amount that is greater or equal to some $\delta > 0$. Since V_h approaches infinity near the boundary of U_h due to radial unboundedness, another function $V_{h'}$ is guaranteed to exist because the collection $\{U_h\}_{h\in\mathcal{N}}$ covers the entire manifold. The combination between this switching logic and gradient-based feedback renders the reference trajectory globally asymptotically stable, which constitutes the first contribution of the work presented in this paper. Figure 1 represents the proposed controller architecture. The proposed controller is not subject to the topological obstructions that hinder continuous feedback and, since the closed-loop system is shown to satisfy the hybrid basic conditions [38, Assumption 6.5], the global asymptotic stability property is robust to small measurement noise. We also show that, if each potential function V_h and gradient are bounded from above and below, respectively, by quadratic functions of the norm of the tracking error, then the trajectories of the closed-loop system converge exponentially fast to the reference trajectory. Note that, switching between local coordinate charts renders the control input discontinuous and, to solve this issue, we also propose a dynamical extension to the controller that removes the discontinuities from the control input, possibly at the expense of exponential convergence.

The collection of functions $\{V_h\}_{h\in\mathcal{N}}$ plays a fundamental role in the controller design process and each function V_h in the collection must satisfy two very important properties: its gradient is zero only if the tracking error is zero and there exists an associated transport map in the same sense as in [14]. However, unlike the work in [14], we do provide a construction of the collection $\{V_h\}_{h\in\mathcal{N}}$ satisfying these properties for any smooth manifold $\mathscr{M}$ based on a given smooth atlas for the manifold.

Remark 1. *Each smooth manifold can be properly embedded in a higher dimensional Euclidean space ([39, Whitney's Embedding Theorem]) and every compact manifold has a finite smooth atlas. However, it may not be clear to the practitioner which representations to use. For example, the Special Orthogonal group of order three can be embedded in a 9-dimensional Euclidean space in the form of rotation matrices, but it can also be embedded in 6-dimensional and even 5-dimensional spaces (c.f. [40]). Moreover, there are multiple finite smooth atlas of* $\mathsf{SO}(3)$*, but the particular choice must be made by the practitioner, depending on the application at hand.*

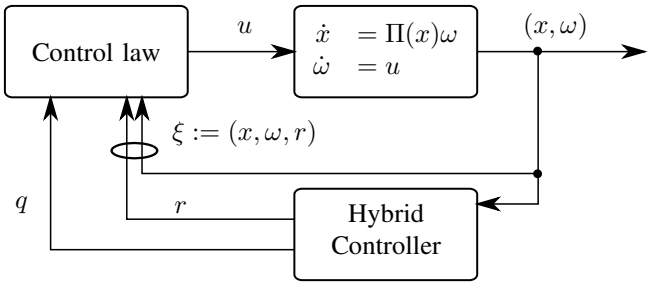

Fig. 1. Structure of the controller presented in Section III-B. The hybrid controller generates a twice differentiable reference trajectory r and updates the logic variable h according to the switching logic given in (8). The control law is given in (12).

In addition, we illustrate the application of the proposed controller to the cases of dynamical systems evolving on the sphere, the unit-quaternion group and the special orthogonal group of order 3. Moreover, we show that the proposed strategy can be also used for global obstacle avoidance in the plane and for global synchronization on the circle which, to the best of our knowledge, constitutes a novel contribution of this paper.

A preliminary version of this paper was presented at the 56th IEEE Conference on Decision and Control (c.f. [41]), without the exponential convergence result, the dynamic extension, the application of the proposed controller to reference tracking on the sphere nor the unit-quaternion group.

D. Organization

In Section II, we present the notation and definitions that are used throughout the paper. Section III presents the controller design and it is split into 5 subsections. The most important results of Section III can be found in Sections III-A through III-C, including the problem setup and the proof of global asymptotic stability for the zero tracking error set. Section III-C presents an exponential convergence result under additional conditions on the Lyapunov function. Section III-E presents an extension to the main controller design of Sections III-A through III-C that moves discontinuities of the control signal from the input to internal variables of the controller and Section III-F presents a construction of potential functions and transport maps that satisfies the conditions of the hybrid controllers that are presented in the preceding sections. In Section IV, we present the application of the proposed controller to trajectory tracking on the 2-dimensional sphere, the unit-quaternion group and the special orthogonal group of order 3, and we illustrate the behavior

This article has been accepted for publication in a future issue of this journal, but has not been fully edited. Content may change prior to final publication. Citation information: DOI 10.1109/TAC.2019.2927708, IEEE Transactions on Automatic Control

of the closed-loop systems by means of simulations. In Sections IV-D and IV-E, we present the application of the proposed control strategy to the problems of obstacle avoidance and global synchronization on the circle, respectively. In Section V, we end the paper with some concluding remarks.

II. Notation & Preliminaries

A. Notation

In this paper, $\mathbb{R}^n$ denotes the n-dimensional Euclidean space equipped with the norm $|x| := \sqrt{x^\top x}$ for each $x \in \mathbb{R}^n$. The symbol $\mathbb{N}$ denotes the set of natural numbers and zero, the symbol $\mathbb{R}^{m\times n}$ denotes the set of $m \times n$ matrices over the field $\mathbb{R}$ and $\mathbb{R}_{\geq 0}$ denotes the set of nonnegative real numbers. We define the operator $\mathrm{vec} : \mathbb{R}^{m\times n} \to \mathbb{R}^{mn}$ as follows: $\mathrm{vec}(A) := (Ae_1^n, \ldots, Ae_m^n)$ for each $A \in \mathbb{R}^{m\times n}$ and making use of the convention $(u, v) = \begin{bmatrix} u^\top & v^\top \end{bmatrix}^\top$ for each $u \in \mathbb{R}^k$ and $v \in \mathbb{R}^\ell$ for some $k, \ell \in \mathbb{N}$. The $n \times n$ identity matrix is denoted by I_n and the n-dimensional vector of ones is denoted by $1_n \in \mathbb{R}^n$. The derivative of a differentiable matrix function with matrix arguments $F : \mathbb{R}^{m\times n} \to \mathbb{R}^{k\times \ell}$ is given by

$$\mathcal{D}_X F(X) := \frac{\partial \,\mathrm{vec}(F(X))}{\partial \,\mathrm{vec}(X)^\top}. \tag{2}$$

for each $X \in \mathbb{R}^{m\times n}$. We omit the subscript in (2) when the derivative is taken with respect to all arguments of the function F. For the particular case of a scalar function $V : \mathbb{R}^n \to \mathbb{R}$, we make use of the more standard notation $\nabla_x V(x) := (\mathcal{D}_x V(x))^\top$ for each $x \in \mathbb{R}^n$.

B. Hybrid Systems

A hybrid system $\mathcal{H}$ with state space $\mathbb{R}^n$ is defined as follows:

$$\begin{aligned} \dot{\xi} &\in F(\xi) \quad \xi \in C \\ \xi^+ &\in G(\xi) \quad \xi \in D \end{aligned}$$

where $\xi \in \mathbb{R}^n$ is the state, $C \subset \mathbb{R}^n$ is the flow set, $F : \mathbb{R}^n \rightrightarrows \mathbb{R}^n$ is the flow map, $D \subset \mathbb{R}^n$ denotes the jump set, and $G : \mathbb{R}^n \rightrightarrows \mathbb{R}^n$ denotes the jump map. A solution ξ to $\mathcal{H}$ is parametrized by (t, j), where t denotes ordinary time and j denotes the jump time, and its domain $\mathrm{dom}\,\xi \subset \mathbb{R}_{\geq 0} \times \mathbb{N}$ is a hybrid time domain: for each $(T, J) \in \mathrm{dom}\,\xi$, $\mathrm{dom}\,\xi \cap ([0, T] \times \{0, 1, \ldots J\})$ can be written in the form $\cup_{j=0}^{J-1}([t_j, t_{j+1}], j)$ for some finite sequence of times $0 = t_0 \leq t_1 \leq t_2 \leq \cdots \leq t_J$, where $I_j := [t_j, t_{j+1}]$ and the t_j's define the jump times. A solution ξ to a hybrid system is said to be *maximal* if it cannot be extended by flowing nor jumping and *complete* if its domain is unbounded. The projection of solutions onto the t direction is given by $\xi{\downarrow_t}(t) := \xi(t, J(t))$ where $J(t) := \max\{j : (t, j) \in \mathrm{dom}\,\xi\}$. Further details on the hybrid systems framework that we use in this paper can be found in [38]. The distance of a point $\xi \in \mathbb{R}^n$ to a closed set $\mathcal{A} \subset \mathbb{R}^n$ is given by $|\xi|_{\mathcal{A}} := \inf_{y\in\mathcal{A}} |y - \xi|$ and $\mathcal{A}$ is said to be: stable for $\mathcal{H}$ if for every $\epsilon > 0$ there exists $\delta > 0$ such that every solution ξ to $\mathcal{H}$ with $|\xi(0, 0)|_{\mathcal{A}} \leq \delta$ satisfies $|\xi(t, j)|_{\mathcal{A}} \leq \epsilon$ for all $(t, j) \in \mathrm{dom}\,\xi$; globally attractive for $\mathcal{H}$ if each maximal solution ξ is complete and $\lim_{t+j\to\infty} |\xi(t, j)|_{\mathcal{A}} = 0$; globally asymptotically stable for $\mathcal{H}$ if it is both stable and globally attractive for $\mathcal{H}$.

III. Controller Design

A. Reference Trajectories and Basic Assumptions

Given the system (1), the main goal of the controller proposed in this section is to track a reference trajectory that is bounded and sufficiently smooth, as specified in the following definition.

Definition 1. *A C^n-reference trajectory on $U \subset \mathscr{M}$ with $n \in \mathbb{N}\backslash\{0\}$ is a smooth path $t \mapsto (y(t), \upsilon(t)) \in U \times \mathbb{R}^k$ satisfying*

$$\begin{aligned} \dot{y}(t) &= \Pi(y(t))\upsilon(t) \\ \upsilon^{(n-1)}(t) &\in M\mathbb{B} \end{aligned} \tag{3}$$

for all $t \geq 0$ for some $M \geq 0$.

Next, we make an adaptation to the definition of a proper indicator given in [38] which will be useful in stating the assumptions of the controller design.

Definition 2. *Given an open subset U of $\mathscr{M}$, a continuous function $V : U \times U \to \mathbb{R}_{\geq 0}$ is a proper indicator on U if, for each $y \in U$, the following holds:*

1) *$V(x, y) = 0$ if and only if $x = y$;*
2) *$V(x_i, y) \to +\infty$ when $i \to \infty$ if either $|x_i| \to \infty$ or $x_i \to \mathrm{bd}(U)$ for each $y \in U$.*

Next, equipped with the notions of C^n-reference trajectories on $\mathscr{M}$ and proper indicators, we list the remaining assumptions of the controller design.

Assumption 1. *Given a finite set $\mathscr{N}$ with cardinality $N > 0$ and a collection of open subsets $\{U_h\}_{h\in\mathscr{N}}$ of $\mathscr{M}$ satisfying $\cup_{h\in\mathscr{N}} U_h = \mathscr{M}$, for each $h \in \mathscr{N}$, there exists a C^2-reference trajectory on U_h, denoted by $t \mapsto (y_h(t), \upsilon_h(t))$, and a compact subset $\mathscr{R}_h$ of $\mathscr{M} \times \mathbb{R}^k$ which is forward invariant for* (3)*.*

Moreover, the following holds for each $h \in \mathscr{N}$:

1) *there exists a continuously differentiable proper indicator V_h on U_h such that*

$$\Pi(x)^\top \nabla_x V_h(x, y_h) = 0 \tag{4}$$

if and only if $y_h = x$;

2) *if $\upsilon_h(t) \neq 0$ for some measurable subset of $\mathbb{R}_{\geq 0}$, then there exists a continuously differentiable function $(x, y_h) \mapsto \mathcal{T}_h(x, y_h)$ such that*

$$\begin{aligned} \nabla_{y_h} V_h(x, y_h)^\top \Pi(y_h) = \\ -\nabla_x V_h(x, y_h)^\top \Pi(x) \mathcal{T}_h(x, y_h), \end{aligned} \tag{5}$$

for each $(x, y_h) \in U_h \times U_h$. Otherwise, we consider $\mathcal{T}_h(x, y_h) = 0$ for each $(x, y_h) \in U_h \times U_h$.

In Assumption 1, we require that the reference trajectory be sufficiently smooth, so that feedforward terms can be computed and injected into the control input. Also, we require it to be bounded, so that invariance principles can be used in the proof of asymptotic stability. More importantly, note

This article has been accepted for publication in a future issue of this journal, but has not been fully edited. Content may change prior to final publication. Citation information: DOI 10.1109/TAC.2019.2927708, IEEE Transactions on Automatic Control

that the gradient of each proper indicator must be zero if and only if the tracking error is zero and there must be a function $(x, y) \mapsto \mathcal{T}_h(x, y)$ satisfying (5), similar to the transport map in [14]. In Section III-F, we provide functions that satisfy the aforementioned conditions, but the controller design follows next under the assumption of a general finite collection of functions $\{V_h\}_{h\in\mathscr{N}}$.

B. General Hybrid Controller and its Main Properties

Letting

$$r := (y_1, \upsilon_1, \ldots, y_N, \upsilon_N) \in \mathscr{R} := \mathscr{R}_1 \times \ldots \times \mathscr{R}_N \tag{6}$$

represent all reference trajectories under Assumption 1, we define

$$\xi := (x, \omega, r) \in \Xi := \mathscr{M} \times \mathbb{R}^k \times \mathscr{R}.$$

It follows from Assumption 1 that $\mathscr{R} \subset (\mathscr{M} \times \mathbb{R}^k)^N$ is compact. Using $\widetilde{\omega}(h, \xi) := \omega - \mathcal{T}_h(x, y_h)\upsilon_h$ as the velocity tracking error for each (h, ξ) in

$$\mathscr{W} := \{(h, \xi) \in \mathscr{N} \times \Xi : (y_h, x) \in U_h \times U_h\}, \tag{7}$$

we define the hybrid controller

$$\begin{aligned} &\dot{h} = 0 \quad (h, \xi) \in C := \{(h, \xi) \in \mathscr{N} \times \Xi : \mu(h, \xi) \leq \delta\} \\ &h^+ \in g(\xi) := \arg\min\{W(h, \xi) | h \in \mathscr{N}\} \\ &\qquad (h, \xi) \in D := \{(h, \xi) \in \mathscr{N} \times \Xi : \mu(h, \xi) \geq \delta\} \end{aligned} \tag{8}$$

with $\delta > 0$ and

$$\mu(h, \xi) := W(h, \xi) - \min_{p\in\mathscr{N}} W(p, \xi) \tag{9}$$

for each $(h, \xi) \in \mathscr{N} \times \Xi$, where

$$W(h, \xi) := \begin{cases} V_h(x, y_h) + \frac{1}{2}|\widetilde{\omega}(h, \xi)|^2 & \text{if } (h, \xi) \in \mathscr{W} \\ +\infty & \text{otherwise} \end{cases} \tag{10}$$

for each $(h, \xi) \in \mathscr{N} \times \Xi$.

We make use of the following two intermediary results to show that the controller is endowed with some regularity properties that are pivotal for well-posedness of the closed-loop hybrid system and asymptotic stability of the set of zero tracking error, given by

$$\mathcal{A} := \{(h, \xi) \in \mathscr{N} \times \Xi : x = y_h, \omega = \mathcal{T}_h(x, y_h)\upsilon_h\}. \tag{11}$$

Lemma 1. *Under Assumption 1, the following hold:*

1) *The function $(h, \xi) \mapsto W(h, \xi)$ in* (10) *is continuous;*
2) *$\min_{p\in\mathscr{N}} W(p, \xi) < +\infty$ for each $\xi \in \Xi$;*
3) *The function μ in* (9) *is continuous;*
4) *The function g in* (8) *is outer semicontinuous.*

Proof. It follows from Assumption 1 that V_h and $\mathcal{T}_h$ are continuous on $U_h \times U_h$ for each $h \in \mathscr{N}$. Hence, W is continuous on $\mathscr{W}$ in (7) because it is the composition of continuous functions in this domain.

Note that

$$\begin{aligned} (\mathscr{N} \times \Xi)\backslash\mathscr{W} &= \{(h, \xi) \in \mathscr{N} \times \Xi : (y_h, x) \notin U_h \times U_h\} \\ &= \{(h, \xi) \in \mathscr{N} \times \Xi : x \notin U_h\} \end{aligned}$$

because (y_h, υ_h) belongs to a compact subset $\mathscr{R}_h$ of $U_h \times \mathbb{R}^k$, by assumption. Therefore, each sequence $\{(h_i, \xi_i)\}_{i\in\mathbb{N}} \subset \mathscr{W}$ converging to $(\mathscr{N} \times \Xi)\backslash\mathscr{W}$, satisfies $x_i \to \mathrm{bd}(U_{h_i})$ when $i \to \infty$. From Assumption 1, we have that V_h is proper indicator on U_h for each $h \in U_h$, hence $V_{h_i}(x_i, y_{h_i}) \to +\infty$ when $i \to \infty$. The fact that $W(h, \xi) \geq V_h(x, y_h)$ for all $(h, \xi) \in \mathscr{W}$, implies that $W(h_i, \xi_i) \to +\infty$ when $i \to \infty$, which proves the continuity of (10) on $\mathscr{N} \times \Xi$.

Since $\bigcup_{h\in\mathscr{N}} U_h = \mathscr{M}$ and $(y_h, \upsilon_h) \in \mathscr{R}_h \subset U_h \times \mathbb{R}^k$ for each $h \in \mathscr{N}$ by assumption, it follows that, for each $(h, \xi) \notin \mathscr{W}$, there exists $p \in \mathscr{N}$ such that $(p, \xi) \in \mathscr{W}$ and, consequently, $W(p, \xi) < +\infty$. We conclude that $\min_{p\in\mathscr{N}} W(p, \xi) < +\infty$.

Given a sequence $\{\xi_i\}_{i\in\mathbb{N}} \subset \Xi$ that converges to $\xi \in \Xi$, the continuity of $\xi \mapsto \varrho(\xi) := \min_{p\in\mathscr{N}} W(p, \xi)$ is demonstrated by showing that $\{\varrho(\xi_i)\}_{i\in\mathbb{N}}$ converges to $\varrho(\xi)$. In this direction, let $\{p_i\}_{i\in\mathbb{N}} \subset \mathscr{N}$ represent a sequence satisfying $W(p_i, \xi_i) = \varrho(\xi_i)$ for each $i \in \mathbb{N}$. Since $\mathscr{N}$ is compact by assumption, there exists a subsequence $\{p_{i(k)}\}_{k\in\mathbb{N}}$ that converges to some $p \in \mathscr{N}$. If there exists $p^\star \in \mathscr{N}$ such that $W(p^\star, \xi) < W(p, \xi)$, then, by continuity of W, there exists $K \in \mathbb{N}$ such that $W(p^\star, \xi_{i(k)}) < W(p_i, \xi_{i(k)})$ for all $k > K$, which is a contradiction, since $p_i \in g(\xi_i) := \arg\min\{W(p, \xi_i) | p \in \mathscr{N}\}$. We also conclude that $p \in g(\xi)$, from which the outer semicontinuity of g follows. □

We define the control law as follows

$$\begin{aligned} \kappa(h, \xi, \dot{\upsilon}) := -\Pi(x)^\top \nabla_x V_h(x, y_h) - \Psi(\widetilde{\omega}(h, \xi)) \\ + \theta_1(h, \xi, \dot{\upsilon}) \end{aligned} \tag{12}$$

for each $(h, \xi, \dot{\upsilon}) \in \mathscr{W} \times \mathbb{R}^{Nk}$, where $\dot{\upsilon} := (\dot{\upsilon_1}, \ldots, \dot{\upsilon_N}) \in \mathbb{R}^{Nk}$,

$$\theta_1(h, \xi, \dot{\upsilon}) := \mathcal{D}(\mathcal{T}_h(x, y_h)\upsilon_h) \begin{bmatrix} \Pi(x)\omega \\ \Pi(y_h)\upsilon_h \\ \dot{\upsilon_h} \end{bmatrix} \tag{13}$$

for each $(h, \xi, \dot{\upsilon}) \in \mathscr{N} \times \Xi \times \mathbb{R}^{Nk}$ and $\Psi : \mathbb{R}^k \to \mathbb{R}^k$ is a *strongly passive function*, i.e., it is a continuous function $y^\top\Psi(y) \geq 0$ for each $y \in \mathbb{R}^k$, where the equality is verified only when $y = 0$.

Lemma 2. *Let Assumption 1 hold. Then, the function κ in* (12) *is continuous.*

Proof. The function Π is a smooth matrix-valued function on $\mathscr{M}$ by assumption and Ψ is continuous by construction. It follows from Assumption 1 that V_h and $\mathcal{T}_h$ are continuously differentiable for each $h \in \mathscr{N}$, thus κ is continuous because it consists of a combination of these function through sums and multiplications. □

C. Closed-loop System and its Main Properties

The interconnection between the plant (1) and the hybrid controller (8) with the input of the plant assigned to (12), is the closed-loop hybrid system $\mathcal{H} := (C, F, D, G)$ given by

$$\begin{aligned} (\dot{h}, \dot{\xi}) \in F(h, \xi) \quad (h, \xi) \in C \\ (h^+, \xi^+) \in G(h, \xi) \quad (h, \xi) \in D \end{aligned} \tag{14}$$

This article has been accepted for publication in a future issue of this journal, but has not been fully edited. Content may change prior to final publication. Citation information: DOI 10.1109/TAC.2019.2927708, IEEE Transactions on Automatic Control

where C and D are given in (8) and

$$F(h,\xi) := \left\{ \begin{bmatrix} 0 \\ \Pi(x)\omega \\ \kappa(h,\xi,\dot{\upsilon}) \\ F_r(r,\dot{\upsilon}) \end{bmatrix} : \dot{\upsilon} \in (M\mathbb{B})^N \right\} \quad \forall (h,\xi) \in C \tag{15a}$$

$$G(h,\xi) := (g(\xi),\xi) \qquad \forall (h,\xi) \in D \tag{15b}$$

with $F_r(r,\dot{\upsilon}) := (\Pi(y_1)\upsilon_1, \dot{\upsilon_1}, \ldots, \Pi(y_N)\upsilon_N, \dot{\upsilon_N})$, for each $(r,\dot{\upsilon}) \in (\mathscr{M} \times \mathbb{R}^k)^N \times \mathbb{R}^{Nk}$ represents the dynamics of the reference trajectories.

We show next that the closed-loop hybrid system satisfies the hybrid basic conditions [38, Assumption 6.5], which ensure nominal robustness to small measurement noise, followed by the main result of this section: the global asymptotic stability of $\mathcal{A}$ in (11) for the closed-loop hybrid system (14).

Lemma 3. *Let Assumption 1 hold. Then, the closed-loop hybrid system* (14) *satisfies:*

1) *C and D are closed;*
2) *F is outer semicontinuous relative to C, locally bounded relative to C and $F(h,\xi)$ is convex for each $(h,\xi) \in C$;*
3) *G is outer semicontinuous relative to D and locally bounded relative to D.*

Proof. The sets C and D are closed because μ is continuous, as shown in Lemma 1. Since $\mu(h,\xi) < +\infty$ for each $(h,\xi) \in \mathscr{W}$, it follows that $C \subset \mathscr{W}$. From Assumption 1, we have that U_h is open for each $h \in \mathscr{N}$, hence $\mathscr{W}$ is an open neighborhood of C.

Since $M\mathbb{B}$ is compact and convex, we conclude that $(h,\xi) \mapsto M\mathbb{B}$ is outer semicontinuous relative to C, locally bounded relative to C and convex for each $(h,\xi) \in C$. To show that the set-valued map

$$(h,\xi) \mapsto \{(\kappa(h,\xi,\dot{\upsilon}) : \dot{\upsilon} \in (M\mathbb{B})^N\} \tag{16}$$

is outer semicontinuous relative to C, let $\{(h_i,\xi_i)\}_{i\in\mathbb{N}} \subset C$ denote a sequence converging to $(h,\xi) \in C$ and let $\{z_i\}_{i\in\mathbb{N}}$ denote a sequence converging to z that satisfies $z_i \in \{\kappa(h,\xi,\dot{\upsilon}) : \dot{\upsilon} \in (M\mathbb{B})^N\}$ for each $i \in \mathbb{N}$. There exists $a_i \in (M\mathbb{B})^N$ such that $z_i = \kappa(h_i,\xi_i,a_i)$ for each $i \in \mathbb{N}$. Since $a_i \in (M\mathbb{B})^N$ for each $i \in \mathbb{N}$, then there exists a convergent subsequence $\{a_{i_j}\}_{j\in\mathbb{N}}$ of $\{a_i\}_{i\in\mathbb{N}}$ whose limit point a belongs to $(M\mathbb{B})^N$ due to the closeness of this set. It follows that

$$\begin{aligned} \lim_{i\to\infty} z_i = z &\iff \lim_{i\to\infty} \kappa(\xi_i,h_i,a_i) = z \\ &\iff \lim_{j\to\infty} \kappa(\xi_{i_j},h_{i_j},a_{i_j}) = z \\ &\iff \kappa(\xi,h,a) = z \end{aligned}$$

because κ is continuous on $\mathscr{W}$ (as shown in Lemma 2) and $\mathscr{W}$ is a neighborhood of C. Since $a \in (M\mathbb{B})^N$, we conclude that $z \in \{\kappa(h,\xi,\dot{\upsilon}) : \dot{\upsilon} \in (M\mathbb{B})^N\}$, which proves outer semicontinuity of (16) relative to C.

The map (16) is locally bounded relative to C because κ is continuous on C and it is convex for each $(h,\xi) \in C$ because it is an affine function on a convex set. The remaining components of the flow map are single-valued continuous functions on C, thus the properties of outer semicontinuity, local boundedness and convexity also hold.

It follows from Lemma 1 that g is outer semicontinuous, thus G is outer semicontinuous relative to D. It is locally bounded relative to D because g takes values over a finite discrete set, thus concluding the proof. □

Next, we present the main result of this section.

Theorem 1. *Let Assumption 1 hold. Then, the set $\mathcal{A}$ in* (11) *is globally asymptotically stable for the closed-loop hybrid system* (14).

Proof. The derivative of (10) on $\mathscr{W}$ is given by

$$\begin{aligned} \mathcal{D}W(h,\xi)f = \nabla V_h(x,y_h)^\top \begin{bmatrix} \Pi(x)\omega \\ \Pi(y_h)\upsilon_h \end{bmatrix} \\ + \widetilde{\omega}(h,\xi)^\top(\kappa(h,\xi,\dot{\upsilon_h}) - \theta_1(h,\xi,\dot{\upsilon})), \end{aligned}$$

for each $f \in F(h,\xi)$ and $(h,\xi) \in \mathscr{W}$. It follows from (5) and (12) that

$$\mathcal{D}W(h,\xi)f = -\widetilde{\omega}(h,\xi)^\top \Psi(\widetilde{\omega}(h,\xi))$$

for each $f \in F(h,\xi)$ and $(h,\xi) \in \mathscr{W}$. As shown in the proof of Lemma 3, $\mathscr{W}$ is an open neighborhood of C, thus the growth of W is upper bounded during flows by

$$u_c(h,\xi) := \begin{cases} -\widetilde{\omega}(h,\xi)^\top \Psi(\widetilde{\omega}(h,\xi)) & \text{if } (h,\xi) \in C \\ -\infty & \text{otherwise} \end{cases},$$

for each $(h,\xi) \in \mathscr{N} \times \Xi$. By construction of the jump set, we have that the growth of W is upper bounded during jumps by

$$u_d(h,\xi) := \begin{cases} -\delta & \text{if } (h,\xi) \in D \\ -\infty & \text{otherwise} \end{cases}$$

for each $(h,\xi) \in \mathscr{N} \times \Xi$. Since W is continuous and (14) satisfies the hybrid basic conditions, as proved in Lemmas 1 and 3, respectively, it follows from [38, Theorem 8.2] that each precompact solution approaches the largest weakly invariant subset of

$$V_h^{-1}(c) \cap \mathrm{cl}(u_c^{-1}(0)) \tag{17}$$

for some $c \in \mathbb{R}$, which is $\mathcal{A}$. To see this, note that each solution ϕ in the largest weakly invariant set of (17) satisfies $\widetilde{\omega}(t,j) := \widetilde{\omega}(h(t,j),\xi(t,j)) = 0$ for each $(t,j) \in \mathrm{dom}\,\phi$, hence, for each $j \in \mathbb{N}$ such that $I^j := \{t : (t,j) \in \mathrm{dom}\,\phi\}$ has nonempty interior, the following holds

$$\frac{d}{dt}\widetilde{\omega}(t,j) = 0 \tag{18}$$

for almost all $t \in I^j$. From (18), (14) and (12), it follows that

$$\Pi(x(t,j))^\top \nabla_x V_{h(t,j)}(x(t,j), y_{h(t,j)}(t,j)) = 0$$

for all $(t,j) \in \mathrm{dom}\,\phi$. It follows from Assumption 1 that $x(t,j) = y_{h(t,j)}(t,j)$ for all $(t,j) \in \mathrm{dom}\,\phi$.

Global pre-asymptotic stability of $\mathcal{A}$ for (14) follows from [38, Theorem 8.8] because $\mathcal{A}$ is compact and W is positive definite relative to $\mathcal{A}$. Completeness of solutions follows

This article has been accepted for publication in a future issue of this journal, but has not been fully edited. Content may change prior to final publication. Citation information: DOI 10.1109/TAC.2019.2927708, IEEE Transactions on Automatic Control

from [38, Proposition 6.10], because: the Viability Condition (VC) is verified, the condition [38, Proposition 6.10.b)] is not verified because every sublevel set of W is bounded and forward invariant and condition [38, Proposition 6.10.c)] is not verified because $C \cup D = \mathscr{N} \times \Xi$, thus $G(D) \subset C \cup D$. □

Since the closed-loop hybrid system satisfies the hybrid basic conditions, it is possible to show that the asymptotic stability of $\mathcal{A}$ is endowed with robustness to perturbations and measurement noise using the tools that are provided in [38, Chapter 7].

D. Guaranteeing Semiglobal Exponential Convergence by Design

Global asymptotic stability, however, fails to supply information about the rate of convergence to the desired reference, since the zero tracking error of a solution ϕ to (14) is only achieved as $t + j \to +\infty$ with $(t, j) \in \operatorname{dom} \phi$. We also show that, if the the following properties are satisfied, then there exists a Lyapunov function that converges to zero exponentially fast.

Assumption 2. *Assumption 1 holds and, for each $h \in \mathscr{N}$ and each compact set $\Lambda \subset U_h \times U_h$, there exist $\bar{b}, \underline{b} > 0$ such that*

$$\left|\Pi(x)^\top \nabla_x V_h(x, y)\right|^2 \geq \underline{b} V_h(x, y) \tag{19a}$$

$$\left|\nabla_x V_h(x, y)\right|^2 \leq \bar{b} V_h(x, y) \tag{19b}$$

for each $(x, y) \in \Lambda$.

Proposition 1. *Given $\underline{\epsilon}_\omega > 0$, let $\Psi(\widetilde{\omega}) := \underline{\epsilon}_\omega \widetilde{\omega}$ for each $\widetilde{\omega} \in \mathbb{R}^k$ and suppose that Assumption 2 holds. Then, for each compact set $\Omega \subset \mathscr{M} \times \mathbb{R}^k$, there exist $\lambda, \epsilon > 0$ such that, for each maximal solution ϕ to the closed-loop hybrid system* (14) *from $\mathscr{N} \times \Omega \times \mathscr{R}$, the following hold:*

1) If $\phi(0, 0) \in C$, then

$$W_\epsilon(\phi(t, j)) \leq W_\epsilon(\phi(0, 0)) \exp(-\lambda t) \tag{20}$$

for each $(t, j) \in \operatorname{dom} \phi$;

2) Otherwise,

$$W_\epsilon(\phi(t, j)) \leq W_\epsilon(\phi(0, 1)) \exp(-\lambda t) \tag{21}$$

for each $(t, j) \in \operatorname{dom} \phi \backslash \{(0, 0)\}$;

where

$$W_\epsilon(h, \xi) := W(h, \xi) + \epsilon \widetilde{\omega}(h, \xi)^\top \Pi(x)^\top \nabla_x V_h(x, y_h) \tag{22}$$

for each $(h, \xi) \in \mathscr{N} \times \Xi$.

Proof. If $\phi(0, 0) \notin C$, then $\phi(0, 0) \in D$, because $C \cup D = \mathscr{N} \times \Xi$. Since ϕ is a maximal solution to (14), it follows that $(0, 1) \in \operatorname{dom} \phi$. Since $G(D) \subset C \backslash D$, it suffices to show point number 1. It follows from Theorem 1 that, for each initial condition $\phi(0, 0) \in C$, $\operatorname{rge} \phi \subset \Omega_W(W(\phi(0, 0)))$ where

$$\Omega_W(\ell) := \{(h, \xi) \in \mathscr{N} \times \Xi : W(h, \xi) \leq \ell\}$$

for each $\ell \in \mathbb{R}$. Since $W(\phi(0, 0)) < +\infty$ for each $\phi(0, 0) \in C$, it follows from the assumption that V_h is a proper indicator on U_h for each $h \in \mathscr{N}$ that $\Omega_W(W(\phi(0, 0)))$ is compact.

Note that

$$W_\epsilon(h^+, \xi^+) \leq W_\epsilon(h, \xi) - \delta + \epsilon \Delta(\phi(0, 0)) \tag{23}$$

for each $(h, \xi) \in \Omega_W(W(\phi(0, 0))) \cap D$ and each $(h^+, \xi^+) \in G(h, \xi)$ with

$$\begin{aligned}\Delta(\phi(0, 0)) := \max\{&\widetilde{\omega}(h, \xi)^\top \Pi(x)^\top \nabla_x V_p(x, y_p) \\ &- \widetilde{\omega}(h, \xi)^\top \Pi(x)^\top \nabla_x V_h(x, y_h) : \\ &(h, \xi) \in \Omega_W(W(\phi(0, 0))), p \in g(\xi)\}.\end{aligned}$$

for each $\phi(0, 0) \in C \cap (\mathscr{N} \times \Omega \times \mathscr{R})$. It follows from (23) that selecting $\epsilon > 0$ satisfying

$$\epsilon \leq \min\left\{\frac{\delta}{\Delta(\phi(0, 0))} : \phi(0, 0) \in C \cap (\mathscr{N} \times \Omega \times \mathscr{R})\right\} \tag{24}$$

implies that W_ϵ is nonincreasing during jumps for each solution with initial condition $\phi(0, 0)$ in $C \cap (\mathscr{N} \times \Omega \times \mathscr{R})$.

It remains to show that for each solution ϕ from $C \cap (\mathscr{N} \times \Omega \times \mathscr{R})$, there exists a positive definite matrix $P \in \mathbb{R}^{2 \times 2}$ such that, for each $j \in \mathbb{N}$ for which $I^j := \{t : (t, j) \in \operatorname{dom} \phi\}$ has nonempty interior, we have that

$$\begin{aligned}&\mathcal{D} W_\epsilon(\phi(t, j)) \frac{d}{dt} \phi(t, j) \leq \\ &-\begin{bmatrix}\sqrt{V_{h(t,j)}(x(t, j), y_{h(t,j)})} \\ |\widetilde{\omega}(t, j)|\end{bmatrix}^\top P \begin{bmatrix}\sqrt{V_{h(t,j)}(x(t, j), y_{h(t,j)})} \\ |\widetilde{\omega}(t, j)|\end{bmatrix}\end{aligned} \tag{25}$$

for almost all $t \in I^j$. To show this, we start by computing the derivative of the cross term in (22) using the derivation rules in [42, Theorem 9] and the flow map definition in (15a), as follows

$$\begin{aligned}&\mathcal{D}\left(\widetilde{\omega}(h, \xi)^\top \Pi(x)^\top \nabla_x V_h(x, y_h)\right) f = \\ &\quad \nabla_x V_h(x, y_h)^\top \Pi(x)(\kappa(h, \xi, \upsilon_h) - \theta_1(h, \xi, \upsilon_h)) \\ &+ \widetilde{\omega}(h, \xi)^\top \big[(\nabla_x V_h(x, y_h)^\top \otimes I_k) \mathcal{D}(\Pi(x)^\top) \Pi(x) \omega \\ &\qquad + \Pi(x)^\top (\mathcal{D}_x(\nabla_x V_h(x, y_h)) \Pi(x) \omega \\ &\qquad\quad + \mathcal{D}_{y_h}(\nabla_x V_h(x, y_h)) \Pi(y_h) \upsilon_h)\big]\end{aligned} \tag{26}$$

for each $(h, \xi) \in C$ and each $f \in F(h, \xi)$, where $\otimes$ denotes the Kronecker product. Next, we split the computation into different parts that correspond to different components of (26), in order to match the construction in (25).

Using the fact that $\operatorname{vec}(ABC) = (C^\top \otimes A) \operatorname{vec}(B)$ for each group of matrices A, B, C whose product ABC is well-defined, it follows that

$$\begin{aligned}&(\nabla_x V_h(x, y_h)^\top \otimes I_k) \mathcal{D}(\Pi(x)^\top) \Pi(x) \omega \\ &\qquad = \mathsf{M}_{k,m}(\mathcal{D}(\Pi(x)^\top) \Pi(x) \omega) \nabla_x V_h(x, y_h),\end{aligned} \tag{27}$$

for each $(h, \xi) \in C$, where $\mathsf{M}_{k,m} : \mathbb{R}^{km} \to \mathbb{R}^{k \times m}$ is such that $\operatorname{vec}(\mathsf{M}_{k,m}(z)) = z$ for each $z \in \mathbb{R}^{mn}$. From (12) and the assumption that $\Psi(\widetilde{\omega}) := \underline{\epsilon}_\omega \widetilde{\omega}$ for each $\widetilde{\omega} \in \mathbb{R}^k$, it follows that

$$\begin{aligned}&\nabla_x V_h(x, y_h)^\top \Pi(x)(\kappa(h, \xi, \upsilon_h) - \theta_1(h, \xi, \upsilon_h)) \\ &\qquad = -\nabla_x V_h(x, y_h)^\top \Pi(x) \Pi(x)^\top \nabla_x V_h(x, y_h) \\ &\qquad\quad - \underline{\epsilon}_\omega \nabla_x V_h(x, y_h)^\top \Pi(x) \widetilde{\omega}(h, \xi)\end{aligned} \tag{28}$$

This article has been accepted for publication in a future issue of this journal, but has not been fully edited. Content may change prior to final publication. Citation information: DOI 10.1109/TAC.2019.2927708, IEEE Transactions on Automatic Control

for each $(h,\xi) \in C$. It follows from Assumption 1 that V_h is twice differentiable, thus

$$\begin{aligned}&\mathcal{D}_{y_h}(\nabla_x V_h(x,y_h))\Pi(y_h)\upsilon_h \\ &\quad = \left(\mathcal{D}_x(\nabla_{y_h} V_h(x,y_h)\Pi(y_h)\upsilon_h)\right)^\top\end{aligned}$$

for each $(h,\xi) \in C$. From (5) it follows that

$$\begin{aligned}&\mathcal{D}_x(\mathcal{D}_{y_h}(V_h(x,y_h))\Pi(y_h)\upsilon_h) \\ &= -\left(\mathcal{D}_x(\nabla_x(V_h(x,y_h)))\Pi(x)\mathcal{T}_h(x,y_h)\upsilon_h\right)^\top \\ &\quad -\left(\mathcal{D}_x(\Pi(x)\mathcal{T}_h(x,y_h)\upsilon_h)\nabla_x V_h(x,y_h)\right)^\top\end{aligned} \tag{29}$$

for each $(h,\xi) \in C$. Replacing (27), (28) and (29) into (26) yields

$$\begin{aligned}&\mathcal{D}\left(\widetilde{\omega}(h,\xi)^\top \Pi(x)^\top \nabla_x V_h(x,y_h)\right) f \\ &= -\nabla_x V_h(x,y_h)^\top \Pi(x)\Pi(x)^\top \nabla_x V_h(x,y_h) \\ &- \underline{\epsilon}_\omega \nabla_x V_h(x,y_h)^\top \Pi(x)\widetilde{\omega}(h,\xi) \\ &+ \widetilde{\omega}(h,\xi)^\top \mathsf{M}_{k,m}(\mathcal{D}(\Pi(x))\Pi(x)\omega)\nabla_x V_h(x,y_h) \\ &+ \widetilde{\omega}(h,\xi)^\top \Pi(x)^\top \mathcal{D}_x(\nabla_x V_h(x,y_h))\Pi(x)\widetilde{\omega}(h,\xi) \\ &- \widetilde{\omega}(h,\xi)^\top \Pi(x)^\top \mathcal{D}_x(\Pi(x)\mathcal{T}_h(x,y_h)\upsilon_h)\nabla_x V_h(x,y_h)\end{aligned}$$

for each $f \in F(h,\xi)$ and $(h,\xi) \in C$. It follows from Assumption 2 that, for each solution ϕ from $C \cap (\mathscr{N} \times \Omega \times \mathscr{R})$, (25) holds with

$$P := \begin{bmatrix} \underline{b}\epsilon & -\frac{\sqrt{\bar{b}}}{2}\epsilon\gamma_{12} \\ -\frac{\sqrt{\bar{b}}}{2}\epsilon\gamma_{12} & \underline{\epsilon}_\omega - \epsilon\left|\gamma_2\right| \end{bmatrix}$$

with

$$\begin{aligned}\gamma_{12} := \max\{&\sigma_{max}(\mathsf{M}_{k,m}(\mathcal{D}(\Pi(x))\Pi(x)\omega) - \underline{\epsilon}_\omega \Pi(x)^\top \\ &- \Pi(x)^\top \mathcal{D}_x(\Pi(x)\mathcal{T}_h(x,y_h)\upsilon) : \\ &(h,\xi) \in \Omega_W(W(0,0)), \phi(0,0) \in C \cap (\mathscr{N} \times \Omega \times \mathscr{R})\}\end{aligned} \tag{30a}$$

$$\begin{aligned}\gamma_2 := \max\{&\lambda_{max}(\Pi(x)^\top \mathcal{D}_x(\nabla_x V_h(x,y_h))\Pi(x)) : \\ &(h,\xi) \in \Omega_W(W(0,0)), \phi(0,0) \in C \cap (\mathscr{N} \times \Omega \times \mathscr{R})\},\end{aligned} \tag{30b}$$

where $\sigma_{max}(A)$ represents the highest singular value of a matrix A and $\lambda_{max}(P)$ represents the eigenvalue of P with largest real part. Selecting ϵ satisfying (24) and

$$\epsilon < \frac{\underline{b}\underline{\epsilon}_\omega}{\underline{b}\left|\gamma_2\right| + \frac{\bar{b}}{4}\gamma_{12}^2}$$

we have P positive definite, thus (20) holds with λ equal to the lowest eigenvalue of P. □

Remark 2. *The property that is proved in Proposition 1 can be referred to as semiglobal exponential convergence of $\mathcal{A}$ for* (14)*, because initial conditions are restricted to a compact (but otherwise arbitrary) subset Ω of $\mathscr{N} \times \Xi$ on which the parameters ϵ and λ of* (20) *and* (21) *depend.*

E. Smoothing the Control Input via Dynamic Extension

In order to the remove the discontinuities from the control input, we add a new controller state $\widehat{\theta} := (\widehat{\theta}_1, \widehat{\theta}_2, \widehat{\theta}_3) \in \mathbb{R}^{m+2k}$ where $\widehat{\theta}_1 \in \mathbb{R}^m$, $\widehat{\theta}_2 \in \mathbb{R}^k$ and $\widehat{\theta}_3 \in \mathbb{R}^k$ are estimates of θ_1 in (13),

$$\theta_2(h,\xi) := \nabla_x V_h(x,y_h) \qquad \forall (h,\xi) \in \mathscr{W} \tag{31a}$$

$$\theta_3(h,\xi) := \mathcal{T}_h(x,y_h)\upsilon_h \qquad \forall (h,\xi) \in \mathscr{W} \tag{31b}$$

respectively, with $\mathscr{W}$ given in (7). For the sake of compactness, let

$$\theta(z) := (\theta_1(z), \theta_2(h,\xi), \theta_3(h,\xi)),$$

defined for each $z := (h,\xi,\dot{\upsilon}) \in \mathscr{N} \times \Xi \times \mathbb{R}^{Nk} \in \mathscr{W} \times \mathbb{R}^{Nk} \subset \mathscr{N} \times \Xi \times \mathbb{R}^{Nk}$. The remainder of this section follows closely the structure of Sections III-C with the exception that the controller (8) needs to be modified in order to include a slightly different jump logic as well as the estimator dynamics

$$\begin{aligned}\dot{\widehat{\theta}} = F_{\widehat{\theta}}(\widehat{\theta},z,\ddot{\upsilon}) &:= \mathcal{D}\theta(z) F_z(\widehat{\theta},z,\ddot{\upsilon}) \\ &- \Gamma^{-1}\begin{bmatrix} \widetilde{\omega}(h,\xi) \\ \Pi(x)\widetilde{\omega}(h,\xi) \\ -\Psi(\widetilde{\omega}(h,\xi)) \end{bmatrix} - \widehat{\Psi}(\widehat{\theta} - \theta(z)),\end{aligned} \tag{32}$$

defined for each $(\widehat{\theta},z,\ddot{\upsilon}) \in \mathbb{R}^{m+2k} \times \mathscr{W} \times \mathbb{R}^{Nk} \times \mathbb{R}^{Nk}$, $\Gamma \in \mathbb{R}^{(m+2k)\times(m+2k)}$ is a positive definite matrix, $v \mapsto \Gamma\widehat{\Psi}(v)$ is a strongly passive function for each $v \in \mathbb{R}^{m+2k}$,

$$F_z(\widehat{\theta},\xi,\dot{\upsilon},\ddot{\upsilon}) := (0, \Pi(x)\omega, \widehat{\kappa}(\widehat{\theta},z), F_r(r,\dot{\upsilon}), \ddot{\upsilon}) \tag{33}$$

for each $(\widehat{\theta},\xi,\dot{\upsilon},\ddot{\upsilon}) \in \mathbb{R}^{m+2k} \times \Xi \times \mathbb{R}^{Nk} \times \mathbb{R}^{Nk}$ and

$$\widehat{\kappa}(\widehat{\theta},x,\omega) := \widehat{\theta}_3 - \Psi(\omega - \widehat{\theta}_2) - \Pi(x)^\top \widehat{\theta}_1$$

for each $(\widehat{\theta},x,\omega) \in \mathbb{R}^{m+2k} \times \mathscr{M} \times \mathbb{R}^k$.

Remark 3. *Note that F_z in* (33) *does not depend on h, because we removed the dependence of the control input $u \equiv \widehat{\kappa}(\widehat{\theta},x,\omega)$ on the logic variable. However, the switching is not removed from the controller, but rather moved to the controller internal variables, as it will become clear in the sequel.*

It is possible to verify that Assumption 1 does not enforce the differentiability requirements that are necessary to compute (32), thus we replace Assumption 1 with the next assumption for the purpose of the controller design presented in this section.

Assumption 3. *Given a finite set $\mathscr{N}$ with cardinality $N > 0$ and a collection of open subsets $\{U_h\}_{h\in\mathscr{N}}$ of $\mathscr{M}$ satisfying $\cup_{h\in\mathscr{N}} U_h = \mathscr{M}$, for each $h \in \mathscr{N}$, there exists a C^3-reference trajectory on U_h, denoted by $t \mapsto (y_h(t), \upsilon_h(t), \dot{\upsilon}_h(t))$, and compact subsets $\mathscr{R}_h$ of $\mathscr{M} \times \mathbb{R}^k$ and $\mathscr{V}_h$ of $\mathbb{R}^k$ such that $\mathscr{R}_h \times \mathscr{V}_h$ is forward invariant for* (3)*.*

Moreover, the following holds for each $h \in \mathscr{N}$:

1) *there exists a continuously differentiable proper indicator V_h on U_h such that* (4) *holds if and only if $y_h = x$;*
2) *if $\upsilon_h(t) \neq 0$ for some measurable subset of $\mathbb{R}_{\geq 0}$, then there exists a continuously differentiable function $(x,y_h) \mapsto \mathcal{T}_h(x,y_h)$ such that* (5) *holds for each $(x,y_h) \in U_h \times U_h$. Otherwise, we consider $\mathcal{T}_h(x,y_h) = 0$ for each $(x,y_h) \in U_h \times U_h$.*

This article has been accepted for publication in a future issue of this journal, but has not been fully edited. Content may change prior to final publication. Citation information: DOI 10.1109/TAC.2019.2927708, IEEE Transactions on Automatic Control

Under Assumption 3, we define $\widehat{\Xi} := \mathscr{N} \times \mathscr{M} \times \mathbb{R}^k \times \widehat{\mathscr{R}}$, where $\widehat{\mathscr{R}} := \mathscr{R} \times (\mathscr{V}_1 \times \ldots \times \mathscr{V}_N)$ with $\mathscr{R}$ given in (6), the closed-loop system is given by

$$\begin{aligned} (\dot{\widehat{\theta}}, \dot{z}) &\in \widehat{F}(\widehat{\theta}, z) \quad (\widehat{\theta}, z) \in \widehat{C} \\ (\widehat{\theta}^+, z^+) &\in \widehat{G}(\widehat{\theta}, z) \quad (\widehat{\theta}, z) \in \widehat{D} \end{aligned} \tag{34}$$

where

$$\begin{aligned} \widehat{F}(\widehat{\theta}, z) &:= \left\{ \begin{bmatrix} F_{\widehat{\theta}}(\widehat{\theta}, z, \ddot{v}) \\ F_z(\widehat{\theta}, \xi, \dot{v}, \ddot{v}) \end{bmatrix} : \ddot{v} \in (M\mathbb{B})^N \right\} \\ &\quad \forall (\widehat{\theta}, z) \in \widehat{C} := \{(\widehat{\theta}, z) \in \mathbb{R}^{m+2k} \times \widehat{\Xi} : \widehat{\mu}(\widehat{\theta}, z) \leq \delta\} \\ \widehat{G}(\widehat{\theta}, z) &:= (\widehat{\theta}, g(\xi), \xi, \dot{v}) \\ &\quad \forall (\widehat{\theta}, z) \in \widehat{D} := \{(\widehat{\theta}, z) \in \mathbb{R}^{m+2k} \times \widehat{\Xi} : \widehat{\mu}(\widehat{\theta}, z) \geq \delta\} \end{aligned} \tag{35}$$

with $\delta > 0$,

$$\widehat{\mu}(\widehat{\theta}, z) := \widehat{W}(\widehat{\theta}, z) - \min_{p \in \mathscr{N}} \widehat{W}(\widehat{\theta}, p, \xi, \dot{v})$$

for each $(\widehat{\theta}, z) \in \mathbb{R}^{m+2k} \times \widehat{\Xi}$ and

$$\widehat{W}(\widehat{\theta}, z) := W(h, \xi) + \frac{1}{2}(\widehat{\theta} - \theta(z))^\top \Gamma (\widehat{\theta} - \theta(z)). \tag{36}$$

Theorem 2. *Let Assumption 3 hold. Then, the set*

$$\begin{aligned} \widehat{\mathcal{A}} := \{(\widehat{\theta}, z) \in \mathbb{R}^{m+2k} \times \widehat{\Xi} : x = y_h, \\ \omega = \mathcal{T}_h(x, y_h) v_h, \widehat{\theta} = \theta(z)\} \end{aligned}$$

is globally asymptotically stable for (35)*.*

Proof. The proof of this result follows closely that of Theorem 1, thus it will be abbreviated. The maps $\widehat{F}$ and $\widehat{G}$ are outer semicontinuous and locally bounded relative to $\widehat{C}$ and $\widehat{D}$, respectively. The set $\widehat{F}(\widehat{\theta}, z)$ is convex for each $(\widehat{\theta}, z) \in C$. The growth of (36) is upper bounded during flows by

$$\widehat{u_c}(\widehat{\theta}, z) = \begin{cases} -(\omega - \widehat{\theta}_2)^\top \Psi (\omega - \widehat{\theta}_2) \\ \qquad -(\widehat{\theta} - \theta(z))^\top \widehat{\Psi} (\widehat{\theta} - \theta(z)) \\ \qquad\qquad\qquad \text{if } (\widehat{\theta}, z) \in \widehat{C} \\ -\infty \qquad\qquad\qquad\qquad \text{otherwise} \end{cases}.$$

The growth of (36) is upper bounded during jumps by

$$\widehat{u_d}(\widehat{\theta}, z) := \begin{cases} -\delta & \text{if } (\widehat{\theta}, z) \in \widehat{D} \\ -\infty & \text{otherwise} \end{cases}.$$

Global pre-asymptotic stability of $\widehat{\mathcal{A}}$ for (34) follows from [38, Theorem 8.8] because $\widehat{\mathcal{A}}$ is compact and $\widehat{W}$ is positive definite relative to $\widehat{\mathcal{A}}$. Completeness of solutions follows from [38, Proposition 6.10]. □

Using the controller proposed in this section we are able to smooth out the control input, at the expense of additional controller dynamics and the guaranteed decay rate that is proved in Proposition 1 under Assumption 2.

F. Constructing potential functions from maximal atlases

General as it may be, the controller design provided in the previous sections does not address the construction of proper indicators that satisfy Assumption 1. However, the result provided next demonstrates that, under some mild conditions, constructing functions of V_h and $\mathcal{T}_h$ that satisfy Assumption 2 is fairly straightforward.

Proposition 2. *Given a smooth atlas $\mathscr{A} := \{(U_h, \psi_h)\}_{h \in \mathscr{N}}$ for $\mathscr{M}$, if $\psi_h(U_h) = \mathbb{R}^n$ for each $h \in \mathscr{N}$, then:*

1) The function

$$V_h(x, y) := \frac{1}{2} |\psi_h(x) - \psi_h(y)|^2 \quad \forall (x, y) \in U_h \times U_h \tag{37}$$

is a proper indicator on U_h satisfying (4) *and* (19)*;*

2) The function

$$\begin{aligned} \mathcal{T}_h(x, y) := (\mathcal{D}\psi_h(x)\Pi(x))^\dagger \mathcal{D}\psi_h(y)\Pi(y) \\ \forall (x, y) \in U_h \times U_h \end{aligned} \tag{38}$$

satisfies (5)*, where $A^\dagger$ is the Moore-Penrose generalized inverse of a matrix A as defined in [43, Section 6.1].*

Proof. Following the definition of a smooth atlas given in [39], ψ_h is a diffeomorphism. Therefore, if $\psi_h(x) = \psi_h(y)$, then $x = y$. Moreover, $|\psi_h(x_i)| \to \infty$ when $i \to \infty$ if x_i is a sequence that satisfies $|x_i| \to +\infty$ or $x_i \to \mathrm{bd}(U_h)$ when $i \to \infty$, thus V_h in (37) is a proper indicator on U_h. To see that (4) holds, note that

$$\Pi(x)^\top \nabla_x V_h(x, y) = \Pi(x)^\top (\mathcal{D}\psi_h(x))^\top (\psi_h(x) - \psi_h(y)). \tag{39}$$

It follows from [43, Fact 2.10.14] that

$$\begin{aligned} \mathrm{rank}(\mathcal{D}\psi_h(x)\Pi(x)) = \mathrm{rank}(\mathcal{D}\psi_h(x)) \\ + \dim(\ker(\mathcal{D}\psi_h(x)) \cap \mathrm{Im}(\Pi(x))) \end{aligned} \tag{40}$$

for each $x \in U_h$, where $\ker(A)$ denotes the nullspace of a matrix A and $\dim S$ denotes the dimension of a space S. Since ψ_h is a diffeomorphism, $\mathcal{D}\psi_h(x) : \mathsf{T}_x\mathscr{M} \to \mathbb{R}^n$ is bijective, thus $\mathrm{rank}(\mathcal{D}\psi_h(x)) = n$ and $\ker(\mathcal{D}\psi_h(x)) \cap \mathsf{T}_x\mathscr{M} = \{0\}$. By assumption, we have that $\mathrm{Im}(\Pi(x)) = \mathsf{T}_x\mathscr{M}$, hence $\ker(\mathcal{D}\psi_h(x)) \cap \mathrm{Im}(\Pi(x)) = \{0\}$ and, consequently, $\dim(\ker(\mathcal{D}\psi_h(x)) \cap \mathrm{Im}(\Pi(x))) = 0$. It follows from (40) that $\mathrm{rank}(\mathcal{D}\psi_h(x)\Pi(x)) = \mathrm{rank}(\Pi(x)^\top \mathcal{D}\psi_h(x)^\top) = n$, which is to say that $\Pi(x)^\top \mathcal{D}\psi_h(x)^\top$ has full column rank. Therefore, since ψ_h is a diffeomorphism, (39) is equal to zero if and only if $x = y$. The relation (5) follows from the fact that $\mathcal{D}\psi_h(x)\Pi(x)$ is right invertible for each $x \in U_h$.

For each compact subset Λ of $U_h \times U_h$, the function (37) satisfies (19a) with

$$\begin{aligned} \underline{b} := 2 \min\{\lambda_{min}(\mathcal{D}\psi_h(x)\Pi(x)\Pi(x)^\top \mathcal{D}\psi_h(x)^\top) : \\ (x, y) \in \Lambda\}, \end{aligned}$$

where $\lambda_{min}(A)$ denotes the minimum eigenvalue of A and satisfies (19b) with

$$\bar{b} := 2 \max\{\lambda_{max}(\mathcal{D}\psi_h(x)\mathcal{D}\psi_h(x)^\top) : (x, y) \in \Lambda\}$$

which is nonzero because $\mathcal{D}\psi_h(x)$ has full rank for each $x \in U_h$. □

This article has been accepted for publication in a future issue of this journal, but has not been fully edited. Content may change prior to final publication. Citation information: DOI 10.1109/TAC.2019.2927708, IEEE Transactions on Automatic Control

It is the construction proposed in Proposition 2 that we use for the several simulations that we present in the following sections.

IV. Applications

A. Global tracking on the two-dimensional sphere

In this section, we apply the controller design of Section III to the tracking of a circular trajectory on the two-dimensional sphere, given by

$$\mathbb{S}^2 := \{x \in \mathbb{R}^3 : x^\top x = 1\}$$

which is a properly embedded submanifold of $\mathbb{R}^3$ with dimension 2.

It follows from [39, Proposition 5.38] that the tangent space to $\mathbb{S}^2$ at x is given by $\mathsf{T}_x\mathbb{S}^2 = \ker(\mathcal{D}\Phi(x)) = \{v \in \mathbb{R}^3 : \mathcal{D}\Phi(x)v = 0\}$, with $\Phi(x) := x^\top x$ for each $x \in \mathbb{S}^2$, hence Π in (1) is given by $\Pi(x) = I_3 - xx^\top$ for each $x \in \mathbb{S}^2$. The reference trajectory that we consider for simulation purposes is the solution to

$$\begin{aligned} \dot{y} &= \Pi(y)\upsilon \\ \dot{\upsilon} &= -\Pi(y)\upsilon \end{aligned} \tag{41}$$

with initial condition $y_0 = (1, 0, 0)$, $\upsilon_0 = (0, 1, 0)$, and $\dot{\upsilon}_0 = (-1, 0, 0)$ which is a circular trajectory around the equator.

The atlas $\mathscr{A} := \{(U_h, \psi_h)\}_{h\in\mathscr{N}}$ with $U_h := \mathbb{S}^2\backslash\{(0, 0, h)\}$ and

$$\psi_h(x) := \left(\frac{x_1}{1 - hx_3}, \frac{x_2}{1 - hx_3}\right)$$

for each $x := (x_1, x_2, x_3) \in U_h$ and $h \in \mathscr{N} := \{-1, 1\}$. This atlas satisfies the conditions of Proposition 2, hence the functions (37) and (38) can be used together with the reference (41) to meet Assumption 3.

Figure 2 represents the simulation results of the closed-loop hybrid system, starting from $x_0 = (-1, 0, 0)$ with initial velocity $\omega_0 = (0, 0, 10)$, logic variable $h_0 = 1$, $k_x = 1$ and $\Psi(\widetilde{\omega}) = -\widetilde{\omega}$ for each $\widetilde{\omega} \in \mathbb{R}^3$. The initial estimator state is set to zero and the initial state of the reference trajectory produced by (41) is $(y_{h_0}, \upsilon_{h_0}, \dot{\upsilon}_{h_0}) := (e_1, e_2, -e_1)$. The high initial velocity ω_0 is meant to shoot the state of the system to the north pole $(0, 0, 1)$ in order to induce controller switching. The time stamps T_i for $i \in \{1, 2\}$ identify the times at which the snapshots in Figure 2 are taken.

The star shaped markers in Figure 2 indicate that a number of controller jumps do occur within $t \in [0\ 0.1]$. The hybrid controller with continuous input has some high frequency switching in the beginning of the simulation while the hybrid controller with discontinuous input only experiences a single jump of the logic variable. The high frequency behavior of the hybrid controller with continuous input is a result of a combination of factors, including: high initial velocity ω_0, high initial estimator error and low convergence rate of the estimator. The controller parameters can be tuned to increase performance and reduce the chattering rate, but these simulations demonstrate that stability is not compromised. Moreover, it should be noted that this high frequency switching occurs on the internal variables of the controller rather than the actuator. High frequency switching can be mitigated by increasing the lower bound on the synergy gap δ that triggers switching, possibly at the expense of higher control authority.

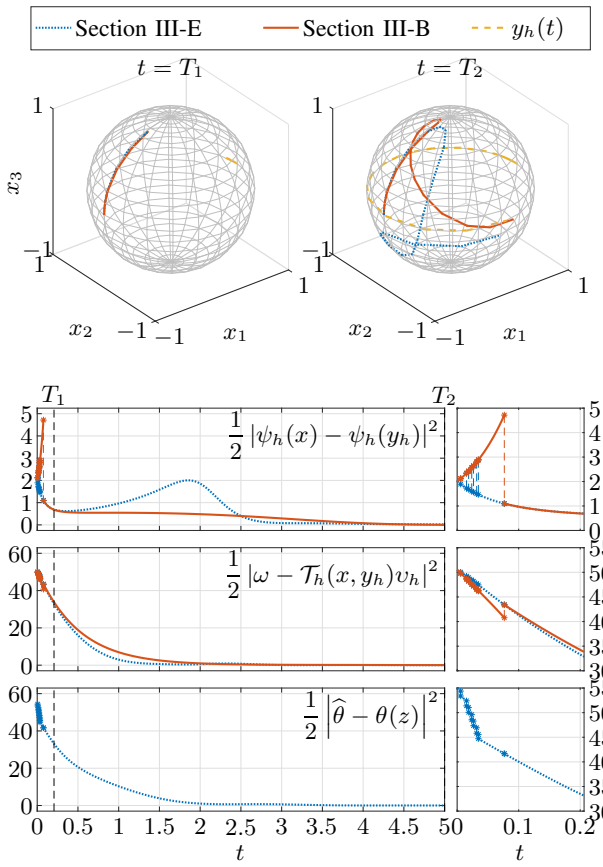

Fig. 2. Simulation of the closed-loop hybrid systems resulting from the interconnection of (1) and the controllers of Sections III-B and III-E for the data provided in Section IV-A. The first row depicts a sequence of snapshots of the state trajectories and reference trajectory at times $T_1 \approx 0.21$ and $T_2 \approx 5.00$. The bottom figures represent the evolution of the tracking and estimation errors with continuous time.

Next, we compare the behavior of the closed-loop hybrid systems of Sections III-B and III-E with the continuous closed-loop system of [14, Lemma 8]. The latter controller consists of a potential function $V(x, y) := 1 - x^\top y$ and a transport map $\mathcal{T}(x, y) := (x^\top y)I_3 + S(y \times x)$, both of which are defined for all $(x, y) \in \mathbb{S}^2 \times \mathbb{S}^2$ with

$$S(x) := \begin{bmatrix} 0 & -x_3 & x_2 \\ x_3 & 0 & -x_1 \\ -x_2 & x_1 & 0 \end{bmatrix}$$

for each $x \in \mathbb{R}^3$. Due to the fact that, V and $\mathcal{T}$ satisfy (5) for all $(x, y) \in \mathbb{S}^2 \times \mathbb{S}^2$, it follows that the set $\mathcal{A}_c := \{(y, \upsilon, x, \omega) \in (\mathbb{S}^2 \times \mathbb{R}^3)^2 : x = y, \omega = \upsilon\}$ is almost globally asymptotically stable for the interconnection between 1 and

$$\begin{aligned} u \equiv \kappa_c(y, \upsilon, x, \omega) := -\Pi(x)\nabla_x V - \Psi(\omega - \mathcal{T}(x, y)\upsilon) \\ + \theta_1(x, y, \upsilon) \end{aligned}$$

for each $(y, \upsilon, x, \omega) \in (\mathbb{S}^2 \times \mathbb{R}^3)^2$. However, if the actuation

This article has been accepted for publication in a future issue of this journal, but has not been fully edited. Content may change prior to final publication. Citation information: DOI 10.1109/TAC.2019.2927708, IEEE Transactions on Automatic Control

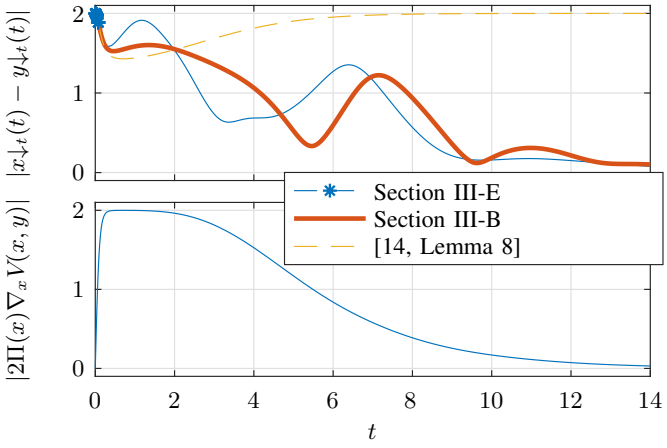

is perturbed by $(1+\sigma)\Pi(x)\nabla_x V(x,y)$ as follows

$$u \equiv \kappa_c(y,\upsilon,x,\omega) + (1+\sigma)\Pi(x)\nabla_x V(x,y)$$

for each $(y,\upsilon,x,\omega) \in (\mathbb{S}^2 \times \mathbb{R}^3)^2$, then the stabilization of $\mathcal{A}_c$ is prevented, as shown in Figure IV-A. In this figure, it is possible to verify that the magnitude of the disturbance converges to 0 with time, but the position error tracking is converging to a nonzero value when the continuous controller is used. On the other hand, the tracking error under the hybrid controllers is converging to 0 despite the influence of the disturbance.

B. Rigid-body stabilization by hybrid unit-quaternion feedback

The stabilization of a rigid-body by hybrid feedback was introduced in [31], but it is explored here nonetheless to illustrate the application of the proposed strategy in the stabilization of multiple points. The dynamics of a rigid-body vehicle can be described by

$$\begin{aligned} \dot{R} &= RS(\Omega) \\ J\dot{\Omega} &= S(J\Omega)\Omega + \tau \end{aligned} \tag{42}$$

where $R \in \mathsf{SO(3)} := \{R \in \mathbb{R}^{3\times 3} : R^\top R = I_3,\ \det(R) = 1\}$ represents the orientation of the vehicle, $\Omega \in \mathbb{R}^3$ is the angular velocity, $\tau \in \mathbb{R}^3$ is the input torque.

Alternatively, the orientation can be represented by an unit-quaternion

$$q := (\eta, \epsilon) \in \mathbb{S}^3 := \{q \in \mathbb{R}^4 : q^\top q = 1\},$$

where $\eta \in \mathbb{R}$ and $\epsilon \in \mathbb{R}^3$ are the scalar and vector components of $q \in \mathbb{S}^3$, using the function

$$\mathcal{R}(q) := I_3 + 2\eta S(\epsilon) + 2S(\epsilon)^2 \quad \forall q \in \mathbb{S}^3. \tag{43}$$

The set $\mathbb{S}^3$ and the function (43) constitute a double cover of $\mathsf{SO(3)}$ because $R(q) = R(-q)$ for each $q \in \mathbb{S}^3$. Moreover, for each solution $t \mapsto (R(t), \Omega(t))$ to (44) for all $t \geq 0$, there exists $q_0 \in \mathbb{S}^3$ satisfying $\mathcal{R}(q_0) = R(0)$ such that the solution $t \mapsto (q(t), \Omega(t))$ to

$$\begin{aligned} \dot{q} &= \frac{1}{2}\begin{bmatrix} -\epsilon^\top \\ \eta I_3 + S(\epsilon) \end{bmatrix}\Omega \\ J\dot{\Omega} &= S(J\Omega)\Omega + \tau \end{aligned} \tag{44}$$

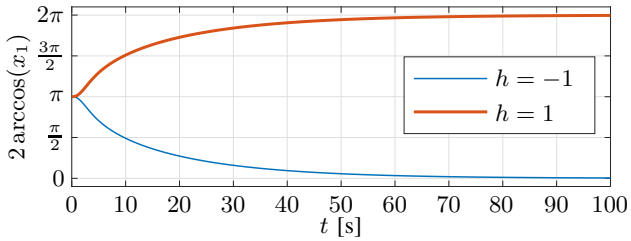

Fig. 3. Representation of the evolution of the rotation angle with time for two different initial values of the logic variable h.

with initial condition q_0 satisfies $\mathcal{R}(q(t)) = R(t)$ for all $t \geq 0$.

Given a reference $t \mapsto (q_r(t), \Omega_r(t)) = (\eta_r(t), \epsilon_r(t), \Omega_r(t))$ satisfying

$$\begin{aligned} \dot{q}_r &= \frac{1}{2}\begin{bmatrix} -\epsilon_r^\top \\ \eta_r I_3 + S(\epsilon_r) \end{bmatrix}\Omega_r \\ J\dot{\Omega}_r &= S(J\Omega_r)\Omega_r + \tau_r \end{aligned}$$

for some $t \mapsto \tau_r(t)$ for all $t \geq 0$, we define the tracking error

$$x := q_r . q^{-1} \tag{45}$$

with dynamics given by (1) and the group product given by

$$q_1 . q_2 := \left(\eta_1\eta_2 - \epsilon_1^\top\epsilon_2, \eta_1\epsilon_2 + \eta_2\epsilon_1 + S(\epsilon_1)\epsilon_2\right)$$

$\omega = q.\nu(\Omega_r - \Omega).q^{-1}$, $\nu(\Omega) = (0, \Omega)$ for each $\Omega \in \mathbb{R}^3$, and

$$\Pi(x) := \frac{1}{2}\begin{bmatrix} -x_2 & -x_3 & -x_4 \\ x_1 & -x_4 & x_3 \\ x_4 & x_1 & -x_2 \\ -x_3 & x_2 & x_1 \end{bmatrix}$$

for each $x = (x_1, x_2, x_3, x_4) \in \mathbb{S}^3$, using the input torque

$$\tau := \mathcal{R}(q)^\top(J(\dot{\Omega}_r + S(\Omega)\Omega_r - u) - S(J\Omega))\Omega, \tag{46}$$

where $u \in \mathbb{R}^3$ is the new virtual input. In this setting, the tracking problem reduces to the problem of asymptotic stabilization of either $y_{-1} := (1,0)$ or $y_1 := (-1,0)$.

Similar to the construction in Section IV-A, a maximal atlas of $\mathbb{S}^3$ is given by $\mathscr{A} := \{(U_h, \psi_h)\}_{h\in\mathscr{N}}$ with $\mathscr{N} := \{-1, 1\}$, $U_h := \mathbb{S}^3\backslash\{(h,0)\}$ and

$$\psi_h(x) := \left(\frac{x_2}{1-hx_1}, \frac{x_3}{1-hx_1}, \frac{x_4}{1-hx_1}\right)$$

for each $x := (x_1, x_2, x_3, x_4) \in U_h$. Note that Assumption 1 is satisfied for the static reference trajectories $y_{-1} := (1,0)$ or $y_1 := (-1,0)$.

Noting that the rotation angle corresponding to the unit-quaternion $x \in \mathbb{S}^3$ in (45) is given by $\theta(x) = 2\arccos(x_1)$ for each $x \in \mathbb{S}^2$, then Figure 3 represents the evolution of the rotation angle for two simulations that correspond to different initializations of the logic variable h with the same initial condition $x(0,0) = \begin{bmatrix}0 & 1 & 0 & 0\end{bmatrix}^\top$, $\omega(0,0) := 0$, which belongs to the set of rotations by an angle equal to π. It is straightforward to verify that the trajectories of the closed-loop system (14) converge to setpoints that map to the identity element of $\mathsf{SO(3)}$ through (43) along two different directions of rotation while the rotation axis remains constant.

This article has been accepted for publication in a future issue of this journal, but has not been fully edited. Content may change prior to final publication. Citation information: DOI 10.1109/TAC.2019.2927708, IEEE Transactions on Automatic Control

C. Rigid-body stabilization by hybrid rotation matrix feedback

In this section, we apply the hybrid control strategy outlined in Section III to global asymptotic tracking of a reference satisfying (42). Similarly to the quaternion-based controller that was presented in Section IV-B, given a reference $t \mapsto (R_r(t), \Omega_r(t))$ that satisfies

$$\begin{aligned} \dot{R}_r &= R_r S(\Omega_r) \\ J\dot{\Omega}_r &= S(J\Omega_r)\Omega_r + \tau_r \end{aligned} \tag{47}$$

for some $t \mapsto \tau_r(t)$ for all $t \geq 0$, we define the tracking error as

$$x := \mathrm{vec}(R_r R^\top) \tag{48}$$

and aim to stabilize the static reference $y := \mathrm{vec}(I_3)$.

To construct an atlas of $\mathsf{SO(3)}$ that satisfies Assumption 1, we make use of the Cayley transform, which is the map $\mathsf{C} : \mathfrak{so}(3) \to \mathsf{SO(3)}$ given by $\mathsf{C}(X) := (I_3 - X)(I_3 + X)^{-1}$, for each $X \in \mathfrak{so}(3) := \{X \in \mathbb{R}^{3\times 3} : X^\top = -X\}$, with inverse $\mathsf{C}^{-1}(R) := (I_3 + R)^{-1}(I_3 - R)$, for each $R \in U := \{R \in \mathsf{SO(3)} : R + I_3 \text{ is nonsingular}\}$. The set U corresponds to the set of all rotation matrices minus the rotations by $180\,\mathrm{deg}$. To see this, let us introduce the *Rodrigues' rotation formula* [44], given by

$$\begin{aligned} \mathcal{R}(v,\theta) :=& \exp(\theta S(v)) \\ =& I_3 + \sin(\theta) S(v) + (1 - \cos(\theta)) S(v)^2 \end{aligned} \tag{49}$$

for each $(v, \theta) \in \mathbb{S}^2 \times [0, \pi]$. Since the eigenvalues of a rotation matrix have unitary norm, if $R + I_3$ is singular, then the eigenvalues of R are $\lambda_1 = 1$ and $\lambda_2 = \lambda_3 = -1$, which implies that $\mathrm{tr}(R) = -1$. Using (49), it follows that $\mathrm{tr}(\mathcal{R}(v,\theta)) = -1$ if and only if $\cos\theta = -1$, thus we conclude that

$$\mathsf{SO(3)} \backslash U := \{R \in \mathbb{R}^{3\times 3} : R = 2vv^\top - I_3 \text{ for some } v \in \mathbb{S}^2\}.$$

Using the Cayley transform, it is possible to construct a smooth atlas for $\mathsf{SO(3)}$ which satisfies Assumption 3, as shown next.

Proposition 3. *Let* $U_0 := U$, $U_h := \{R \in \mathbb{R}^{3\times 3} : \mathcal{R}(e_h, \pi/2)R \in U\}$ *for each* $h \in \{1,2,3\}$, *and*

$$\begin{aligned} \psi_0(R) &:= S^{-1}(\mathsf{C}^{-1}(R)) && \forall R \in U_0 \\ \psi_h(R) &:= S^{-1}(\mathsf{C}^{-1}(\mathcal{R}(e_h, \pi/2)R)) && \forall R \in U_h \end{aligned}$$

for each $h \in \{1,2,3\}$, *then* $\mathscr{A} := \{(U_i, \psi_i)\}_{i\in\mathscr{N}}$ *with* $\mathscr{N} := \{0,1,2,3\}$ *is a maximal atlas for* $\mathsf{SO(3)}$ *and* $\psi_h(U_h) = \mathbb{R}^3$ *for each* $h \in \mathscr{N}$.

Proof. It follows from the fact that C^{-1} and S^{-1} are diffeomorphisms from $\mathfrak{so}(3)$ to $\mathsf{SO(3)}$ and from $\mathfrak{so}(3)$ to $\mathbb{R}^3$, respectively, that $\psi_h(U_h) = \mathbb{R}^3$ for each $h \in \mathscr{N}$. The proof that $\mathscr{A}$ is a maximal atlas for $\mathsf{SO(3)}$ follows closely the one in [45]: it can be shown that the subset of $\mathsf{SO(3)}$ that does not belong to $U_0 \cup U_1$ is given by

$$\begin{aligned} \mathsf{SO(3)} \backslash (U_0 \cup U_1) = \{&R \in \mathbb{R}^{3\times 3} : \exists v \in \mathbb{S}^2 \\ &R = 2vv^\top - I_3, v^\top e_1 = 0\}. \end{aligned}$$

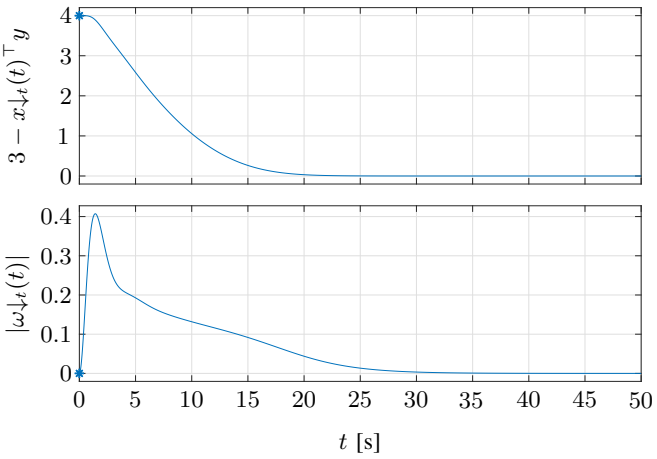

Fig. 4. Evolution of the orientation and angular velocity errors.

Similarly, the subset of $\mathsf{SO(3)}$ that does not belong to $U_0 \cup U_1 \cup U_2$ is given by

$$\begin{aligned} \mathsf{SO(3)} \backslash (U_0 \cup U_1 \cup U_2) = \{&R \in \mathbb{R}^{3\times 3} : \exists v \in \mathbb{S}^2 \\ &R = 2vv^\top - I_3, v^\top e_1 = v^\top e_2 = 0\}, \end{aligned}$$

which is a singleton $\mathsf{SO(3)} \backslash (U_0 \cup U_1 \cup U_2) = \{2e_3 e_3^\top - I_3\}$ that belongs to U_3. □

Defining $\mathsf{M}_{m,n} : \mathbb{R}^{mn} \to \mathbb{R}^{m\times n}$ as the function that satisfies $\mathrm{vec}\,\mathsf{M}_{m,n}(x) = x$ for each $x \in \mathbb{R}^{mn}$, it follows from (42) and (47) that the evolution of the tracking error (48) is described by (1) with $\omega = R(\Omega_r - \Omega)$ and $x \to \Pi(x)$ given by

$$\Pi(x) := \begin{bmatrix} E_1(\mathsf{M}_{3,3}(x)) & E_2(\mathsf{M}_{3,3}(x)) & E_3(\mathsf{M}_{3,3}(x)) \end{bmatrix}$$

for each $x \in \mathbb{R}^9$, with $E_i(R) := -\mathrm{vec}(RS(e_i))$ for each $i \in \{1,2,3\}$, using the input transformation

$$\tau := R^\top (J(\dot{\Omega}_r + S(\Omega)\Omega_r - u) - S(J\Omega)\Omega),$$

which is identical to (46).

Figure 4 represents the evolution of the orientation and angular velocity errors for the initial condition $x(0,0) := \mathrm{vec}(2n_0 n_0^\top - I_3)$, $\omega(0,0) := 0$ for the closed-loop hybrid system (14) with $\delta = 1$.

D. Global Obstacle Avoidance on the Plane

In this section, let us consider the problem of global asymptotic stabilization of the origin of

$$\dot{z} = \omega, \quad \dot{\omega} = u \tag{50}$$

with state $(z, \omega) \in \mathbb{R}^2 \times \mathbb{R}^2$ and input $u \in \mathbb{R}^2$, in the presence of an obstacle that is contained within a closed ball centered at $z_0 \in \mathbb{R}^2$ with radius $\epsilon > 0$, denoted by $z_0 + \epsilon\mathbb{B} := \{z \in \mathbb{R}^2 : |z - z_0| \leq \epsilon\}$, satisfying $|z_0| > \epsilon$ so that it does not contain the origin.

The presence of the obstacle implies that the state variable z is constrained to $\mathbb{R}^2 \backslash (z_0 + \epsilon\mathbb{B})$ which is an open submanifold of $\mathbb{R}^2$. The key to solve the given problem

This article has been accepted for publication in a future issue of this journal, but has not been fully edited. Content may change prior to final publication. Citation information: DOI 10.1109/TAC.2019.2927708, IEEE Transactions on Automatic Control

using the tools that are presented in this paper lies in the observation that $\mathbb{R}^2\backslash(z_0+\epsilon\mathbb{B})$ is diffeomorphic to $\mathbb{R}\times\mathbb{S}^1$ with $\mathbb{S}^1:=\{x\in\mathbb{R}^2:x^\top x=1\}$ through the diffeomorphism

$$f(z):=\begin{bmatrix}\log(|z-z_0|-\epsilon)\\ \dfrac{z-z_0}{|z-z_0|}\end{bmatrix}\quad\forall z\in\mathbb{R}^2\backslash(z_0+\epsilon\mathbb{B}).$$

Using $x:=f(z)$ as the new state variable, the dynamics of the plant are given by

$$\begin{aligned}\dot{x}&=\mathcal{D}f(f^{-1}(x))\omega\\ \dot{\omega}&=u\end{aligned}\tag{51}$$

which match (1) with $\Pi(x)=\mathcal{D}f(f^{-1}(x))$ for each $x\in\mathbb{R}\times\mathbb{S}^1$. In the sequel, we follow the controller design that was presented in Section III-B using the construction of Section III-F.

A smooth atlas $\mathscr{A}:=\{(U_h,\psi_h)\}_{h\in\mathscr{N}}$ of $\mathbb{R}\times\mathbb{S}^1$ can be built from the chart $(\mathbb{R},\mathrm{id})$ for $\mathbb{R}$ where id is the identity function and from the stereographic projection on the circle as follows:

$$\psi_h(x):=\left(x_1,\frac{x_2}{1+hx_3}\right)$$

for each $x:=(x_1,x_2,x_3)\in U_h$ with $h\in\mathscr{N}:=\{-1,1\}$ and $U_h:=\{x\in\mathbb{R}\times\mathbb{S}^1:x_3\neq -h\}$. This smooth atlas is suitable to the problem at hand provided that the center of the obstacle $z_0=(z_{0,1},z_{0,2})\in\mathbb{R}^2$ does not satisfy $z_{0,1}=0$. In that case, a different stereographic projection must be selected. For the simulation results presented in this section, we have selected $z_0=(1,0)$ and $\epsilon=1/2$.

Figure 5 represents the two solutions to the closed-loop system in z-coordinates starting from the same initial condition for z, but different values of the logic variable. The reference trajectory is a constant obtained from f as follows:

$$y_h(t)=f(0)\qquad\forall t\geq 0\tag{52}$$

for each $h\in\mathscr{N}$ and we have selected $\delta=1$ and $\Psi(\widetilde{\omega})=-\widetilde{\omega}$ for each $\widetilde{\omega}\in\mathbb{R}^2$. It is possible to verify that both trajectories converge to the origin but the direction in which they circumvent the obstacle depends on the initialization of the hybrid controller. The figure also depicts the region of the state space where either control law can be selected depending on the initialization of the controller and this region separates the regions where only one of the control laws is allowed. This prevents chattering due to arbitrarily small noise at the expense of slightly larger rotations around the obstacle.

Remark 4. *In this section, we have selected a constant reference trajectory* (52) *for illustration purposes. However, we could consider more complex reference trajectories generated by an exosystem given by a copy of the plant* (50) *with some assigned input.*

E. Global Synchronization on $\mathbb{S}^1$

Consider the dynamics of K agents belonging to $\mathbb{S}^1:=\{x\in\mathbb{R}^2:x^\top x=1\}$, given by

$$\dot{x}_i=Sx_i\Omega_i,\quad\dot{\Omega}_i=w_i$$

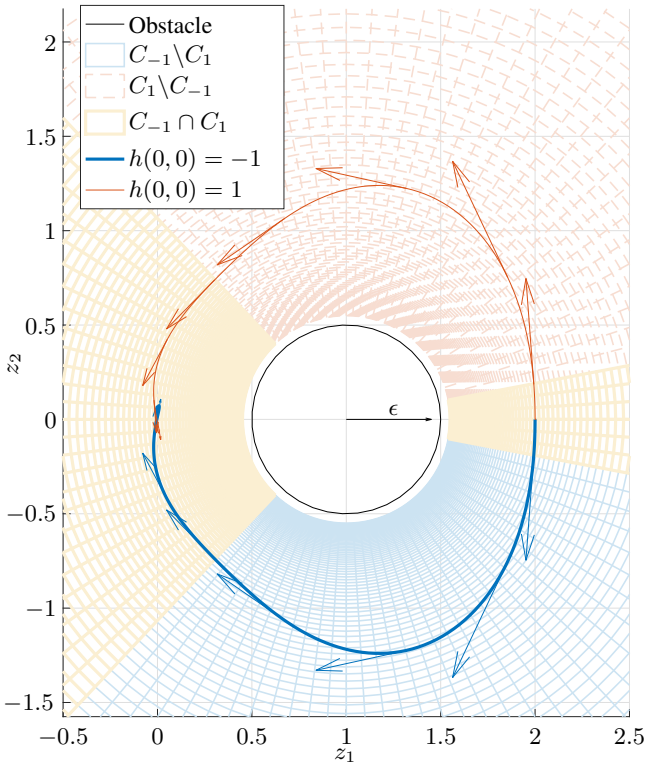

Fig. 5. Representation in the z-plane of two solutions to the closed-loop system resulting from the interconnection between (51) and the controller proposed in Section IV-D for different initial values of the logic variable. The sets C_{-1} and C_1 represent the projection of the flow set onto the z-plane for values of the logic variable $h=-1$ and $h=1$, respectively. More specifically, we have $C_h:=\{z\in\mathbb{R}^2:(f(z),h,0)\in C\}$ for each $h\in\mathscr{N}$ and, to be perfectly clear, if z belongs to $C_h\backslash C_{-h}$ then the control law associated with h is selected. On the other hand, if z belongs to $C_{-1}\cap C_1$ then either control law can be selected depending on the initial condition.

where $S:=\begin{bmatrix}0&-1\\1&0\end{bmatrix}$ and $x_i\in\mathbb{S}^1$, $\Omega_i\in\mathbb{R}$, $w_i\in\mathbb{R}$ denote the position, velocity and input of the agent $i\in\{1,2,\ldots,K\}$, respectively.

We say that the agents are synchronized if $x_i=x_j$ for all $i,j\in\{1,2,\ldots,K\}$, thus they remain synchronized by collective rotations; i.e., for each $R\in\mathsf{SO}(2):=\{R\in\mathbb{R}^{2\times 2}:R^\top R=I_2,\det(R)=1\}$, if $x_i=x_j$, then $Rx_i=Rx_j$. This suggests that the synchronization problem is best described in the quotient manifold $(\mathbb{S}^1)^K/\mathsf{SO}(2)$, which is derived from the action of $\mathsf{SO}(2)$ on $(\mathbb{S}^1)^K$ and has the properties presented next.

Lemma 4. *The left Lie group action of* $\mathsf{SO}(2)$ *on* $(\mathbb{S}^1)^K$ *is given by*

$$R\cdot x:=(Rx_1,Rx_2,\ldots,Rx_K)\quad\forall(R,x)\in\mathsf{SO}(2)\times(\mathbb{S}^1)^K\tag{53}$$

with $x:=(x_1,\ldots,x_K)$ *and it acts smoothly, freely and properly on* $(\mathbb{S}^1)^{K-1}$.

Proof. The Lie group action (53) is smooth and free because the isotropy group is trivial for each $x\in(\mathbb{S}^1)^K$. It follows from [39, Corollary 21.6] that it is proper. □

It follows directly from Lemma 4 and from [39, The-

This article has been accepted for publication in a future issue of this journal, but has not been fully edited. Content may change prior to final publication. Citation information: DOI 10.1109/TAC.2019.2927708, IEEE Transactions on Automatic Control

orem 21.10] that $(\mathbb{S}^1)^K/\mathsf{SO}(2)$ is a $(K-1)$-dimensional smooth manifold with a unique smooth structure that renders the quotient map π_R a smooth submersion, where

$$\pi_R : (\mathbb{S}^1)^K \to (\mathbb{S}^1)^K/\mathsf{SO}(2) \tag{54}$$

maps each point $x \in (\mathbb{S}^1)^K$ to its equivalence class $[x] \in (\mathbb{S}^1)^K/\mathsf{SO}(2)$ under the action (53). This corresponds to the orbit of x, denoted by $\mathsf{SO}(2)\cdot x$, and given by $\pi_R^{-1}([x]) = \mathsf{SO}(2)\cdot x := \{R\cdot x : R \in \mathsf{SO}(2)\}$.

Furthermore, suppose that each agent corresponds to a vertex in V of a connected and undirected tree graph $\mathsf{G} := (\mathsf{V}, \mathsf{E})$ such that each edge in E represents the communication constraints between agents in the network. Given an orientation σ of G[1], the incidence matrix B of the oriented graph $\mathsf{G}^\sigma := (\mathsf{V}, \mathsf{E}^\sigma)$ is a matrix with rows and columns indexed by the vertices and edges of G, respectively, such that the ij-entry of B is equal to 1 if the vertex i is the head of the edge j, -1 if it is the tail of j, and 0 otherwise (c.f. [46, Chapter 8.3]). It turns out that the incidence matrix is instrumental in the characterization of the tangent space to $(\mathbb{S}^1)^K/\mathsf{SO}(2)$.

Lemma 5. *Let π_R denote the quotient map given in* (54)*. Given a connected and undirected graph $\mathsf{G} := (\mathsf{V}, \mathsf{E})$ and an orientation σ of G, we have that*

$$\mathrm{Im}(\Pi(x)) = \mathsf{T}_{\pi_R(x)}\big((\mathbb{S}^1)^K/\mathsf{SO}(2)\big)$$

for each $x \in (\mathbb{S}^1)^K$, where $\Pi(x) := \mathcal{S}(x)B$ with

$$\mathcal{S}(x) := \begin{bmatrix} Sx_1 & 0 & \dots & 0 \\ 0 & Sx_2 & \ddots & \vdots \\ \vdots & \ddots & \ddots & 0 \\ 0 & \dots & 0 & Sx_K \end{bmatrix} \tag{55}$$

for each $x \in (\mathbb{S}^1)^K$, and $B \in \mathbb{R}^{K\times(K-1)}$ denotes the incidence matrix of the oriented graph G^σ.

Proof. The tangent space to $\mathsf{SO}(2)\cdot x$ is given by

$$\mathsf{T}_x(\mathsf{SO}(2)\cdot x) = \{a(Sx_1, \dots, Sx_K) : a \in \mathbb{R}\}.$$

We have that

$$\begin{bmatrix}(Sx_1)^\top & \dots & (Sx_K)^\top\end{bmatrix}\Pi(x) = -1_K^\top B = 0$$

where 1_K is a K-dimensional vector of ones, hence $\mathsf{T}_x(\mathsf{SO}(2)\cdot x)$ is orthogonal to $\mathrm{Im}(\Pi(x))$. Noting that $\mathrm{Im}(\mathcal{S}(x)) = \mathsf{T}_x(\mathbb{S}^1)^K$, it follows that

$$\begin{aligned}\mathrm{Im}(\Pi(x)) &= \mathsf{T}_x(\mathbb{S}^1)^K/\mathsf{T}_x(\mathsf{SO}(2)\cdot x)\\ &= \mathsf{T}_{\pi_R(x)}\big((\mathbb{S}^1)^K/\mathsf{SO}(2)\big).\end{aligned}$$

because $\mathsf{T}_x(\mathsf{SO}(2)\cdot x)$ is the nullspace of $\mathcal{D}\pi_R(x)$ (c.f. [39, Proposition 5.38]). □

[1]An arc is an ordered pair of adjacent vertices of a graph G and an orientation σ is a function that maps each arc to $\{-1, 1\}$ such that, if (u, v) is an arc of G, then $\sigma(u, v) = -\sigma(u, v)$. If $\sigma(u, v) = 1$, then u is the tail of the edge and v is its head.

Global synchonization on the circle is then defined as the global asymptotic stabilization of

$$\begin{aligned}\mathcal{A} := \{(h, x, \omega) \in \mathscr{N} \times (\mathbb{S}^1)^K \times \mathbb{R}^{K-1} : \omega = 0,\\ x_i = x_j \text{ for each } i, j \in \{1, 2, \dots, K\}\}\end{aligned} \tag{56}$$

for a closed-loop hybrid system resulting from the interconnection of a hybrid controller with state $h \in \mathscr{N}$ and the dynamical system (1) with $\Pi(x) := \mathcal{S}(x)B$ and $\mathcal{S}$ given in (55). Note that the mismatch between the dimensions in the states x and ω has to do with the fact that there are K vertices in G but only $K-1$ edges.

The design of the hybrid controller follows the construction that was presented in Section III-F. In this direction, we resort to an atlas that is adapted to the $\mathsf{SO}(2)$ action on $(\mathbb{S}^1)^K$. Such an atlas is comprised of cubical charts $(U_p \cap U_h, (\alpha_p, \psi_h))$ with coordinate function $(\alpha_p(x), \psi_h(x)) \in \mathbb{R}\times\mathbb{R}^{K-1}$, such that each orbit intersects $U_p \cap U_h$ either in the empty set or a single slice where ψ_h is constant (c.f. [39, Theorem 21.10]). The collection $\{(U_p, \alpha_p)\}_{p\in\mathscr{N}_p}$ can be taken as an atlas for $\mathbb{S}^1$ that identifies the position of a single agent such as, for example: $U_p := \{x \in (\mathbb{S}^1)^K : x_1 \neq -p\}$, $\alpha_p(x) = x_{1,1}/(1 + px_{1,2})$ for each $x \in (\mathbb{S}^1)^K$ with $x_1 := (x_{1,1}, x_{1,2})$ and $\mathscr{N}_p := \{-1, 1\}$ which identifies the position of x_1. The collection $\{(U_h, \psi_h)\}_{h\in\mathscr{N}}$ identifies the position of each agent relative to each other and can be constructed from G as follows: let $M : \mathsf{E}^\sigma \to \{1, \dots, K-1\}$ denote a bijective map that labels each edge of G^σ, then for each $(i, j) \in \mathsf{E}^\sigma$, we define

$$\psi_h^k(x) := \frac{x_i^\top x_j}{1 + h_k x_i^\top S x_j} \quad \forall x \in U_h$$

with $k = M(i, j)$ and $h := (h_1, \dots, h_{K-1}) \in \mathscr{N} := \{-1, 1\}^{K-1}$ and

$$\begin{aligned}U_h := \{x \in (\mathbb{S}^1)^K : x_i^\top S x_j \neq -h_k,\ k = M(i, j)\\ \text{for some } (i, j) \in \mathsf{E}^\sigma\}.\end{aligned}$$

Letting $\psi_h(x) := (\psi_h^1(x), \dots, \psi_h^{K-1}(x))$, we have that $(\alpha_p(x), \psi_h(x))$ is a smooth bijective function from $U_p \cap U_h$ to $\mathbb{R}^K$ with smooth inverse and, consequently,

$$\{(U_p \cap U_h, (\alpha_p(x), \psi_h(x)))\}_{(p,h)\in\mathscr{N}_p\times\mathscr{N}}$$

is a smooth atlas adapted to the $\mathsf{SO}(2)$ action on $(\mathbb{S}^1)^K$ and, more importantly, $\mathscr{A} := \{(U_h, \psi_h)\}_{h\in\mathscr{N}}$ is a smooth atlas for $(\mathbb{S}^1)^K/\mathsf{SO}(2)$ (c.f [39, Theorem 21.10]). Using the smooth atlas $\mathscr{A}$ for $(\mathbb{S}^1)^K/\mathsf{SO}(2)$, it is possible to use the construction in Section III-F to globally asymptotically stabilize the set (56).

Noting that $\psi_h(y) = 1_{K-1}$ for each $h \in \mathscr{N}$ and considering that the reference trajectory y is a constant corresponding to the equivalence class x satisfying $x_i = x_j$ for all $i, j \in \{1, 2, \dots, K\}$. It is relevant to point out that the degree of freedom corresponding to the collective rotations of the agents is not controlled with this strategy.

To illustrate the controller proposed in this section through simulation results, we resort to a network of three agents represented by a graph $\mathsf{G} := (\mathsf{V}, \mathsf{E})$ with $\mathsf{V} := \{1, 2, 3\}$ and $\mathsf{E} := \{\{1, 2\}, \{2, 3\}\}$. Using the orientation σ defined by

This article has been accepted for publication in a future issue of this journal, but has not been fully edited. Content may change prior to final publication. Citation information: DOI 10.1109/TAC.2019.2927708, IEEE Transactions on Automatic Control

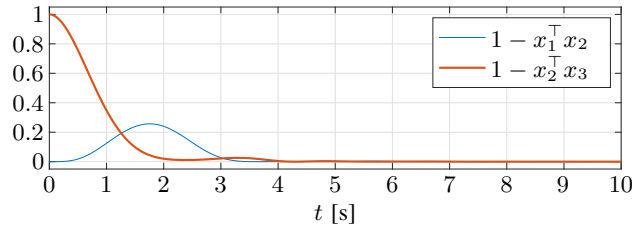

Fig. 6. Evolution of the distance between the agents in G.

$\sigma(1,2) = 1$ and $\sigma(2,3) = 1$ the incidence matrix of G^σ is given by

$$B := \begin{bmatrix} -1 & 0 \\ 1 & -1 \\ 0 & 1 \end{bmatrix}.$$

In this particular case, the atlas $\mathscr{A} := \{(U_h, \psi_h)\}_{h \in \mathcal{N}}$ adapted to the $\mathsf{SO}(2)$ action on $(\mathbb{S}^1)^K$ is given by

$$\psi_h(x) := \left(\frac{x_1^\top x_2}{1 + h_1 x_1^\top S x_2}, \frac{x_2^\top x_3}{1 + h_1 x_2^\top S x_3} \right) \quad \forall x \in U_h$$

with $h := (h_1, h_2)$ and

$$U_h := \{x \in (\mathbb{S}^1)^K : x_1^\top S x_2 \neq -h_1,\ x_2^\top S x_3 \neq -h_2\}.$$

Figure 6 represents the evolution of the distance between the agents in G for a particular simulation of the closed-loop system using the controller proposed in Section III-B using the construction of Section III-F. The initial conditions for this simulation are

$$x_1(0,0) = x_2(0,0) = (1,0) \qquad x_3(0,0) = (0,1)$$
$$h_1(0,0) = h_2(0,0) = 1 \qquad \omega(0,0) = 0$$

and we select $\delta = 1$ and $\Psi(\widetilde{\omega}) = -\widetilde{\omega}$ for each $\widetilde{\omega} \in \mathbb{R}^2$. The initial conditions were selected so as to generate a jump at the beginning of the simulation and, due to the lack of exogenous disturbances, the solution is not subject to further jumps during agent synhronization.

V. Conclusion

In this paper, we presented a hybrid control strategy for the global asymptotic tracking of a reference defined on a smooth manifold. The proposed strategy relies on the switching between local coordinates using a switching logic that guarantees convergence to the desired trajectory. We illustrated the proposed strategy with its application to three different examples: the two-dimensional sphere, the unit-quaternion group and the special orthogonal group. In addition, we also applied the proposed controller to the problems of obstacle avoidance on the plane and synchronization on the circle.

References

[1] F. Bullo and A. D. Lewis, *Geometric Control of Mechanical Systems*. New York, NY: Springer, 2005.

[2] D. Koditschek, "The Application of Total Energy as a Lyapunov Function for Mechanical Control Systems," *Contemporary Mathematics*, vol. 97, pp. 131–157, 1989.

[3] M.-D. Hua, T. Hamel, P. Morin, and C. Samson, "Control of VTOL vehicles with thrust-tilting augmentation," *Automatica*, vol. 52, pp. 1–7, 2015.

[4] A. Tayebi and S. McGilvray, "Attitude stabilization of a VTOL quadrotor aircraft," *IEEE Transactions on Control Systems Technology*, vol. 14, no. 3, pp. 562–571, 2006.

[5] T. Lee, M. Leok, and N. H. McClamroch, "Nonlinear Robust Tracking Control of a Quadrotor UAV on SE(3)," *Asian Journal of Control*, vol. 15, no. 2, pp. 391–408, 2013.

[6] A. P. Aguiar and J. P. Hespanha, "Trajectory-Tracking and Path-Following of Underactuated Autonomous Vehicles With Parametric Modeling Uncertainty," *IEEE Transactions on Automatic Control*, vol. 52, no. 8, pp. 1362–1379, 2007.

[7] E. Lefeber, K. Y. Pettersen, and H. Nijmeijer, "Tracking control of an underactuated ship," *IEEE Transactions on Control Systems Technology*, vol. 11, no. 1, pp. 52–61, 2003.

[8] R. M. Murray, *A Mathematical Introduction to Robotic Manipulation*. CRC press, 1994.

[9] S. Zhao and D. Zelazo, "Bearing Rigidity and Almost Global Bearing-Only Formation Stabilization," *IEEE Transactions on Automatic Control*, vol. 61, no. 5, pp. 1255–1268, 2016.

[10] L. Sun, W. Huo, and Z. Jiao, "Adaptive Backstepping Control of Spacecraft Rendezvous and Proximity Operations with Input Saturation and Full-State Constraint," *IEEE Transactions on Industrial Electronics*, vol. 64, no. 1, pp. 480–492, 2017.

[11] T. Rybus, "Obstacle avoidance in space robotics: Review of major challenges and proposed solutions," *Progress in Aerospace Sciences*, vol. 101, pp. 31–48, 2018.

[12] M. Malisoff, M. Krichman, and E. Sontag, "Global Stabilization for Systems Evolving on Manifolds," *Journal of Dynamical and Control Systems*, vol. 12, no. 2, pp. 161–184, 2006.

[13] E. D. Sontag, "A 'universal' construction of Artstein's theorem on nonlinear stabilization," *Systems & Control Letters*, vol. 13, no. 2, pp. 117–123, 1989.

[14] F. Bullo and R. M. Murray, "Tracking for fully actuated mechanical systems: a geometric framework," *Automatica*, vol. 35, no. 1, pp. 17–34, 1999.

[15] H. K. Khalil, *Nonlinear systems*. Upper Saddle River, NJ: Prentice Hall, 3rd editio ed., 2002.

[16] R. A. Freeman and P. Kokotovic, *Robust Nonlinear Control Design : State-Space and Lyapunov Techniques*. Basel: Birkhauser, 2008.

[17] L. Nicolaescu, *An Invitation to Morse Theory*. Berlin: Springer, 2007.

[18] J.-Y. Wen and K. Kreutz-Delgado, "The attitude control problem," *IEEE Transactions on Automatic Control*, vol. 36, no. 10, pp. 1148–1162, 1991.

[19] A. Sanyal, A. Fosbury, N. Chaturvedi, and D. Bernstein, "Inertia-Free Spacecraft Attitude Tracking with Disturbance Rejection and Almost Global Stabilization," *Journal of Guidance, Control, and Dynamics*, vol. 32, no. 4, 2009.

[20] D. H. S. Maithripala, J. M. Berg, and W. P. Dayawansa, "Almost-global tracking of simple mechanical systems on a general class of Lie groups," *IEEE Transactions on Automatic Control*, vol. 51, no. 2, pp. 216–225, 2006.

[21] P. O. Pereira and D. V. Dimarogonas, "Family of controllers for attitude synchronization on the sphere," *Automatica*, vol. 75, pp. 271–281, jan 2017.

[22] S. P. Bhat and D. S. Bernstein, "A topological obstruction to continuous global stabilization of rotational motion and the unwinding phenomenon," *Systems & Control Letters*, vol. 39, no. 1, pp. 63–70, 2000.

[23] O.-E. Fjellstad and T. Fossen, "Singularity-free tracking of unmanned underwater vehicles in 6 DOF," in *Proceedings of the 33rd IEEE Conference on Decision and Control*, pp. 1128–1133, IEEE, 1994.

[24] N. Chaturvedi and H. McClamroch, "Asymptotic Stabilization of the Inverted Equilibrium Manifold of the 3-D Pendulum Using Non-Smooth Feedback," *IEEE Transactions on Automatic Control*, vol. 54, no. 11, pp. 2658–2662, 2009.

[25] C. G. Mayhew and A. R. Teel, "On the topological structure of attraction basins for differential inclusions," *Systems & Control Letters*, vol. 60, no. 12, pp. 1045–1050, 2011.

[26] D. E. Koditschek and E. Rimon, "Robot navigation functions on manifolds with boundary," *Advances in Applied Mathematics*, vol. 11, no. 4, pp. 412–442, 1990.

[27] R. G. Sanfelice, A. R. Teel, and R. Goebel, "Supervising a Family of Hybrid Controllers for Robust Global Asymptotic Stabilization," in *Proceedings of the 47th Conference on Decision and Control*, pp. 4700–4705, 2008.

[28] C. G. Mayhew, R. G. Sanfelice, and A. R. Teel, "Synergistic Lyapunov functions and backstepping hybrid feedbacks," in *Proceedings of the 2011 American Control Conference*, pp. 3203–3208, 2011.
[29] C. G. Mayhew, R. G. Sanfelice, and A. R. Teel, "Further results on synergistic Lyapunov functions and hybrid feedback design through backstepping," in *Proceedings of the IEEE Conference on Decision and Control*, pp. 7428–7433, IEEE, jun 2011.
[30] C. G. Mayhew and A. R. Teel, "Hybrid control of spherical orientation," in *Proceedings of the 49th IEEE Conference on Decision and Control*, pp. 4198–4203, 2010.
[31] C. G. Mayhew, R. G. Sanfelice, and A. R. Teel, "Quaternion-Based Hybrid Control for Robust Global Attitude Tracking," *IEEE Transactions on Automatic Control*, vol. 56, no. 11, pp. 2555–2566, 2011.
[32] C. G. Mayhew and A. R. Teel, "Synergistic Hybrid Feedback for Global Rigid-Body Attitude Tracking on SO(3)," *IEEE Transactions on Automatic Control*, vol. 58, no. 11, pp. 2730–2742, 2013.
[33] S. Berkane, A. Abdessameud, and A. Tayebi, "Hybrid global exponential stabilization on SO(3)," *Automatica*, vol. 81, pp. 279–285, 2017.
[34] T. Lee, "Global Exponential Attitude Tracking Controls on SO(3)," *IEEE Transactions on Automatic Control*, vol. 60, no. 10, pp. 2837–2842, 2015.
[35] S. Berkane and A. Tayebi, "Construction of Synergistic Potential Functions on SO(3) with Application to Velocity-Free Hybrid Attitude Stabilization," *IEEE Transactions on Automatic Control*, vol. 62, no. 1, 2017.
[36] P. Casau, R. G. Sanfelice, R. Cunha, D. Cabecinhas, and C. Silvestre, "Robust global trajectory tracking for a class of underactuated vehicles," *Automatica*, vol. 58, pp. 90–98, 2015.
[37] R. Sanfelice, M. Messina, S. Emre Tuna, and A. Teel, "Robust hybrid controllers for continuous-time systems with applications to obstacle avoidance and regulation to disconnected set of points," in *Proceedings of the 2006 American Control Conference*, 2006.
[38] R. Goebel, R. G. Sanfelice, and A. R. Teel, *Hybrid Dynamical Systems: Modeling, Stability, and Robustness*. Princeton University Press, 2012.
[39] J. M. Lee, *Introduction to Smooth Manifolds*. Springer, 2nd ed., 2013.
[40] J. Stuelpnagel, "On the parametrization of the three-dimensional rotation group," *SIAM Review*, vol. 6, no. 4, 1964.
[41] P. Casau, R. Cunha, R. G. Sanfelice, and C. Silvestre, "Hybrid Feedback for Global Asymptotic Stabilization on a Compact Manifold," in *Proceedings of the 56th Conference on Decision and Control (CDC)*, (Melbourne), pp. 2384–2389, 2017.
[42] J. R. Magnus and H. Neudecker, "Matrix Differential Calculus with Applications to Simple, Hadamard, and Kronecker Products," *Journal of Mathematical Psychology*, vol. 29, 1985.
[43] D. S. Bernstein, *Matrix Mathematics*. Princeton, NJ: Princeton University Press, 2009.
[44] O. Rodrigues, "Des lois géométriques qui régissent les déplacements d'un système solide dans l'espace, et de la variation des coordonnées provenant de ces déplacements considérés indépendamment des causes qui peuvent les produire," *Journal de mathématiques pures et appliquées*, vol. 1, no. 5, pp. 380–440, 1840.
[45] E. W. Grafarend and W. Kühnel, "A minimal atlas for the rotation group SO(3)," *International Journal on Geomathematics*, vol. 2, no. 1, pp. 113–122, 2011.
[46] C. Godsil and G. F. Royle, *Algebraic Graph Theory*. Graduate Texts in Mathematics, Springer New York, 2001.

Pedro Casau is a Research Assistant at the SCORE Lab of the Faculty of Science and Technology, University of Macau and a Junior Researcher at the Institute for Systems and Robotics, Lisbon, Portugal. He received received the B.Sc. in Aerospace Engineering in 2008 from Instituto Superior Técnico (IST), Lisbon, Portugal. In 2010, he received the M.Sc. in Aerospace Engineering from IST and enrolled in the Electrical and Computer Engineering Ph.D. program at the same institution which he completed with distinction and honours in 2016. While at IST, he participated on several national and international research projects on guidance, navigation and control of unmanned air vehicles (UAVs) and satellites. His current research interests include nonlinear control, hybrid control systems, vision-based control systems, controller design for autonomous air-vehicles.

Rita Cunha received the Licenciatura degree in Information Systems and Computer Engineering and the Ph.D. degree in Electrical and Computer Engineering from the Instituto Superior Técnico (IST), Universidade de Lisboa, Portugal, in 1998 and 2007, respectively. She is an Assistant Professor with the Department of Electrical and Computer Engineering of IST and researcher with Institute for Systems and Robotics in Lisbon. Her research interests include nonlinear systems and control, optimal control, vision-based control, multi-agent systems, with application to the development autonomous robotic vehicles.

Ricardo G. Sanfelice received the B.S. degree in Electronics Engineering from the Universidad de Mar del Plata, Buenos Aires, Argentina, in 2001, and the M.S. and Ph.D. degrees in Electrical and Computer Engineering from the University of California, Santa Barbara, CA, USA, in 2004 and 2007, respectively. In 2007 and 2008, he held postdoctoral positions at the Laboratory for Information and Decision Systems at the Massachusetts Institute of Technology and at the Centre Automatique et Systèmes at the École de Mines de Paris. In 2009, he joined the faculty of the Department of Aerospace and Mechanical Engineering at the University of Arizona, Tucson, AZ, USA, where he was an Assistant Professor. In 2014, he joined the University of California, Santa Cruz, CA, USA, where he is currently Professor in the Department of Electrical and Computer Engineering. Prof. Sanfelice is the recipient of the 2013 SIAM Control and Systems Theory Prize, the National Science Foundation CAREER award, the Air Force Young Investigator Research Award, and the 2010 IEEE Control Systems Magazine Outstanding Paper Award. His research interests are in modeling, stability, robust control, observer design, and simulation of nonlinear and hybrid systems with applications to power systems, aerospace, and biology.

Carlos Silvestre received the Licenciatura degree in Electrical Engineering from the Instituto Superior Tecnico (IST) of Lisbon, Portugal, in 1987 and the M.Sc. degree in Electrical Engineering and the Ph.D. degree in Control Science from the same school in 1991 and 2000, respectively. In 2011 he received the Habilitation in Electrical Engineering and Computers also from IST. Since 2000, he is with the Department of Electrical Engineering of the Instituto Superior Tecnico, where he is currently an Associate Professor of Control and Robotics on leave. Since 2015 he is a Professor of the Department o Electrical and Computers Engineering of the Faculty of Science and Technology of the University of Macau. Over the past years, he has conducted research on the subjects of navigation, guidance and control of air and ocean robots. His research interests include linear and nonlinear control theory, hybrid control, sensor based control, coordinated control of multiple vehicles, networked control systems, fault detection and isolation, and fault tolerant control.